FOUNDATIONS
ADVANCES

Volume 78 (2022)

Supporting information for article:

Vanishing of the atomic form factor derivatives in non-spherical structural refinement – a key approximation scrutinized in the case of Hirshfeld atom refinement

Laura Midgley, Luc J. Bourhis, Oleg V. Dolomanov, Simon Grabowsky, Florian Kleemiss, Horst Puschmann and Norbert Peyerimhoff

Supplementary information for Vanishing of the atomic form factor derivatives in non-spherical structural refinement - A key approximation scrutinised in the case of Hirshfeld Atom Refinement

Laura Midgley, Luc J. Bourhis, Oleg V. Dolomanov, Simon Grabowsky, Florian Kleemiss, Horst Puschmann, Norbert Peyerimhoff

This supplementary information is organised in accordance with the sections of the main article. Largely we present graphs and tables which are useful for understanding and confirming our findings, or are of interest for curiosity's sake, but were not necessary for the main body of the article.

Sections without additional information are omitted.

Contents

1 Details of datasets **S2**

2 The three main refinement procedures **S3**
2.1 Flowcharts side-by-side . . . S3

3 The quality of numerical nonspherical refinement **S4**
3.1 Shift/esd diagrams . . . S4
3.2 wR2 diagrams (ammonia) . . . S6
3.3 wR2 diagrams (epoxide) . . . S10
3.4 wR2 diagrams (L-alanine) . . . S14
3.5 L-Alanine by TAAM . . . S18
3.6 Table 2 . . . S20

4 Comparison of refinement minima **S21**
4.1 Basis set dependence . . . S21

5 Bringing In Uncertainties **S23**
5.1 Ammonia . . . S23
5.2 Epoxide . . . S26
5.3 L-Alanine . . . S30

6 Conclusion & Outlook **S36**
6.1 Neutron data . . . S36

B Uncertainty balls **S41**
B.1 The matrix J for ammonia . . . S41

1 Details of datasets

Table S1: Crystalllographic data for datasets used. Since all data was literature reported we summarize the data from the original sources in combination with the results from numerical refinement.

Compound	**Epoxide** (Grabowsky *et al.*, 2010)	**Ammonia** (Boese *et al.*, 1997)	**L-Alanine** (Destro *et al.*, 1988)
Formula	C_2H_4O	NH_3	$C_3H_7NO_2$
$D_{calc.}/g\ cm^{-3}$	1.162	0.838	1.405
μ/mm^{-1}	0.092	0.064	0.117
Formula Weight	44.053	17.031	89.095
Size/mm^3	0.30×0.30×0.30	not reported	not reported
T/K	100(2)	160(2)	23(2)
Crystal System	monoclinic	cubic	orthorhombic
Space Group	$P2_1/n$	$P2_13$	$P2_12_12_1$
a/Å	4.633(5)	5.1305(8)	5.9279(10)
b/Å	8.400(1)	5.1305(8)	12.2597(17)
c/Å	6.577(3)	5.1305(8)	5.7939(9)
$\alpha°$	90	90	90
$\beta°$	100.37(6)	90	90
$\gamma°$	90	90	90
V/Å^3	251.8(3)	135.05(4)	421.07(11)
Z	4	4	4
Z'	1	0.333333	1
Wavelength/Å	0.71068	0.71069	0.71073
Radiation type	Mo K_α	Mo K_α	Mo K_α
Θ_{min}	3.98	5.62	3.32
Θ_{max}	34.99	29.96	50.14
Measured Refl's.	2081	1762	2519
Indep't Refl's	1109	136	2519
Refl's I≥2 σ(I)	899	133	2393
R_{int}	0.0286	0.0303	0.0000
Parameters	64	13	118
Restraints	0	0	0

2 The three main refinement procedures

2.1 Flowcharts side-by-side

We present here the flow charts for approximate and numerical nonspherical refinements side-by-side to highlight the similarities and differences.

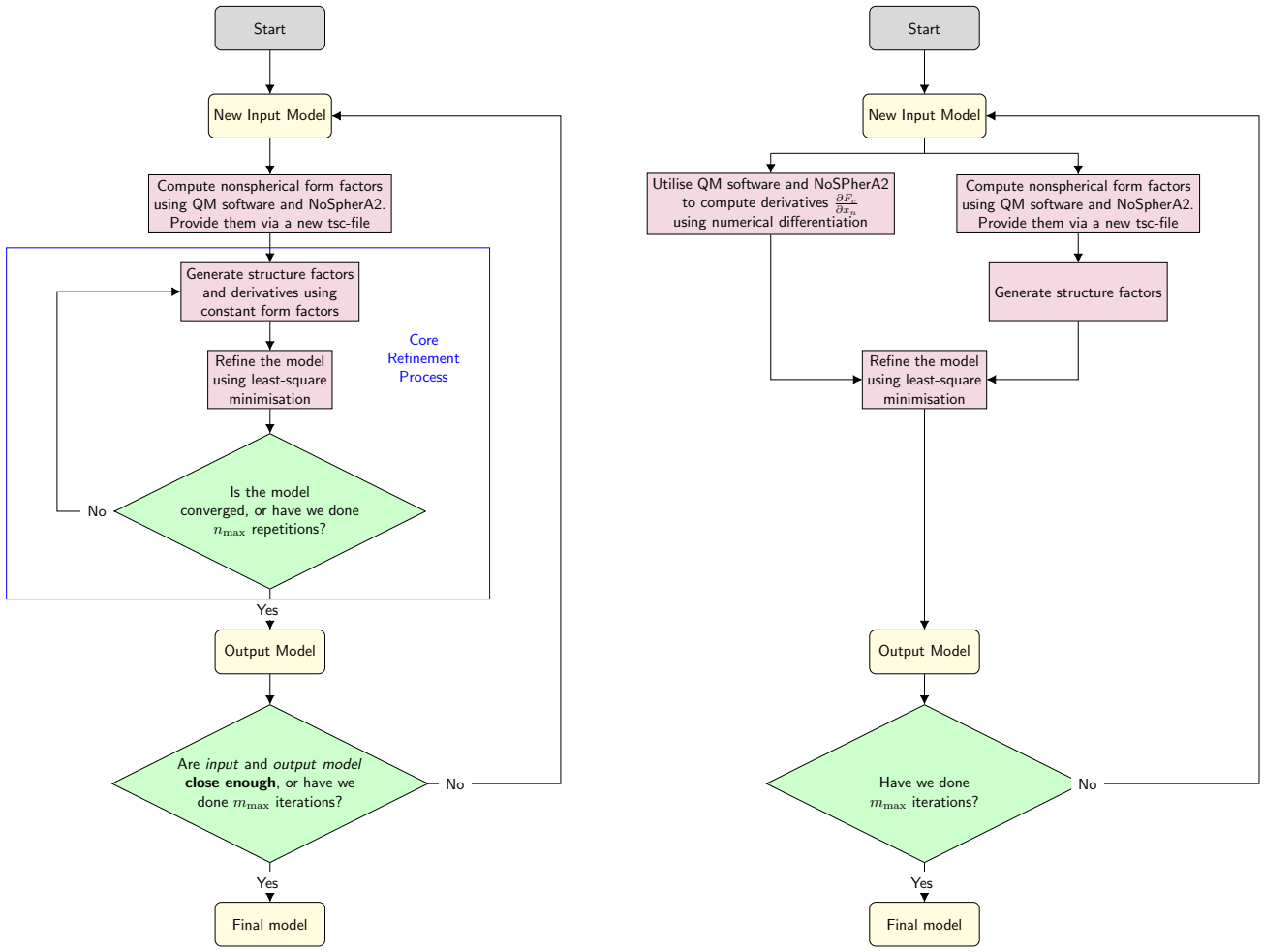

(a) Flow chart illustration of Approximate Nonspherical Refinement

(b) Flow chart illustration of Numerical Nonspherical Refinement

Figure S1: Side-by-side flow charts for approximate and numerical nonspherical refinements

3 The quality of numerical nonspherical refinement

We present graphs for the three molecules (ammonia, epoxide and L-alanine). Figures S2, S3 and S4 show the shift/esd progression for 6 different δ values, and hybrid refinement. Figures S5 to S22 show the progression of wR2 through numerical nonspherical refinement with the different δ, and hybrid, and comparing the progression when starting from $\mathbf{x}_{\text{spher}}$ or $\mathbf{x}_{\text{appr}}$.

3.1 Shift/esd diagrams

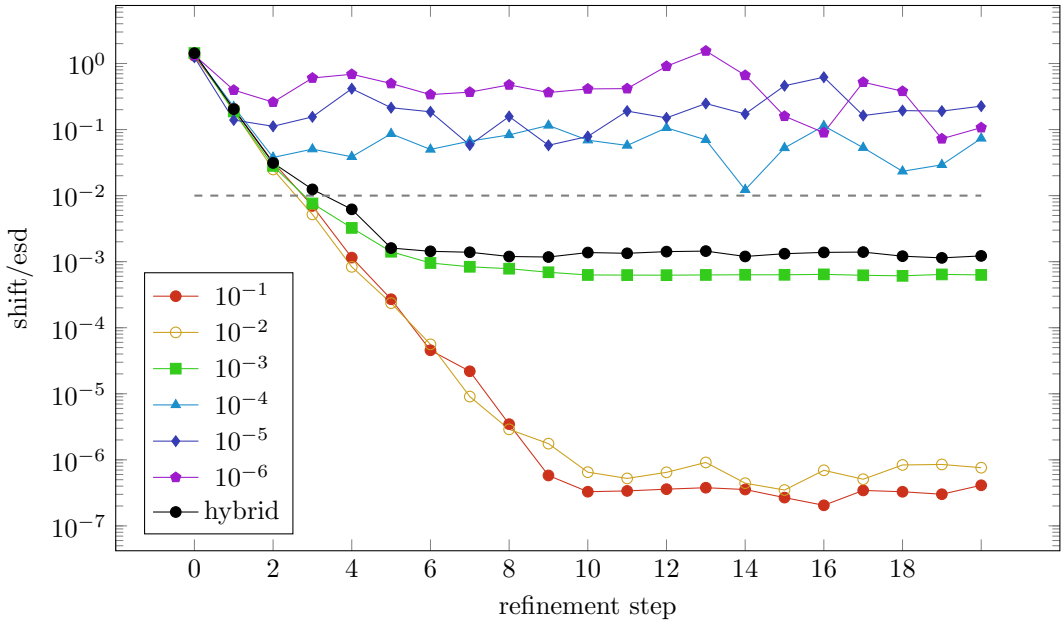

Figure S2: Maximal shift/esd for numerical refinement starting from $\mathbf{x}_{\text{appr}}$ for $\delta = 10^{-1}$, ..., 10^{-6} Å, and hybrid at $\delta = 10^{-3}$ Å (ammonia)

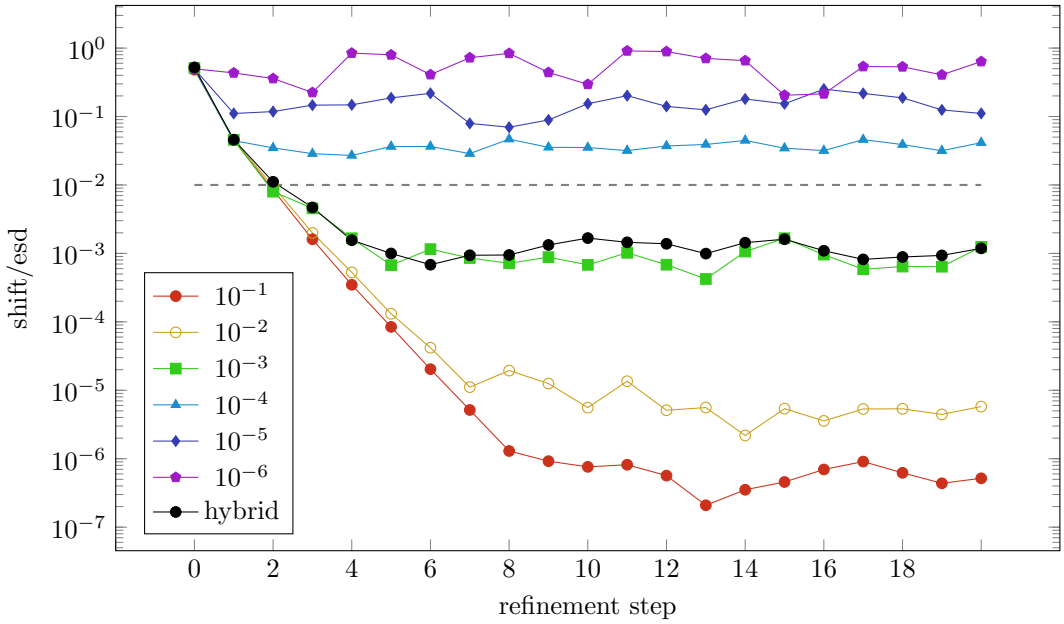

Figure S3: Maximal shift/esd for numerical refinement starting from $\mathbf{x}_{\text{appr}}$ for $\delta = 10^{-1}$, ..., 10^{-6} Å, and hybrid at $\delta = 10^{-3}$ Å (epoxide)

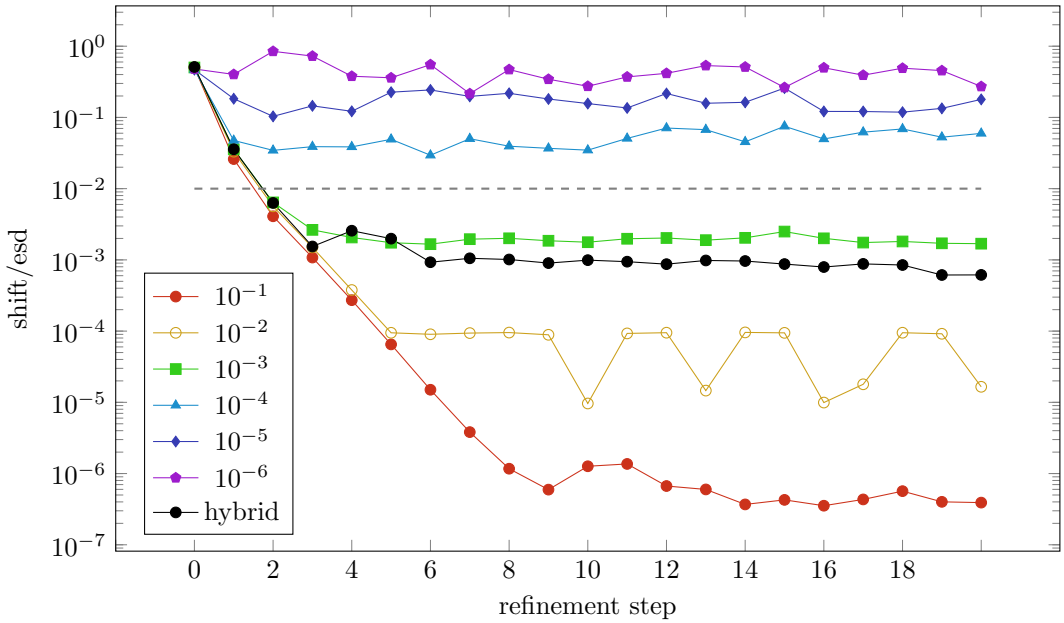

Figure S4: Maximal shift/esd for numerical refinement starting from $\mathbf{x}_{\text{appr}}$ for $\delta = 10^{-1}$, ..., 10^{-6}Å, and hybrid at $\delta = 10^{-3}$ Å (L-alanine)

3.2 wR2 diagrams (ammonia)

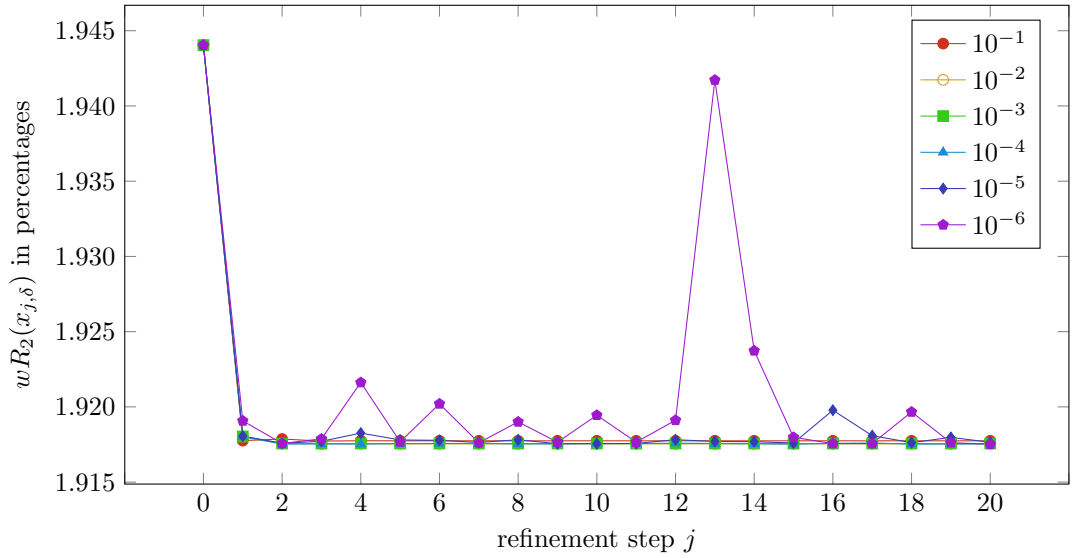

Figure S5: The progression of $wR_2(x_j)$ for $j = 0, 1, \ldots, 20$ and for $\delta = 10^{-1}, \ldots, 10^{-6}$ Å starting from $\mathbf{x}_{\text{appr}}$ (ammonia)

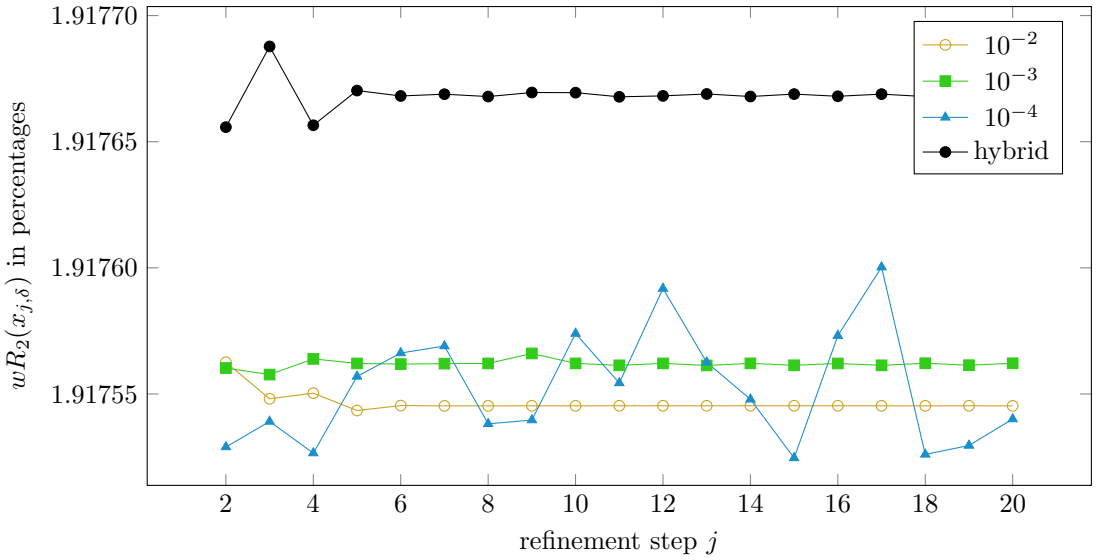

Figure S6: As in Figure S5; the progression of $wR_2(x_j)$ for $j = 2, 3, \ldots, 20$ and for $\delta = 10^{-2}$ Å, 10^{-3} Å, 10^{-4} Å, and hybrid at $\delta = 10^{-3}$ Å starting from $\mathbf{x}_{\text{appr}}$ (ammonia)

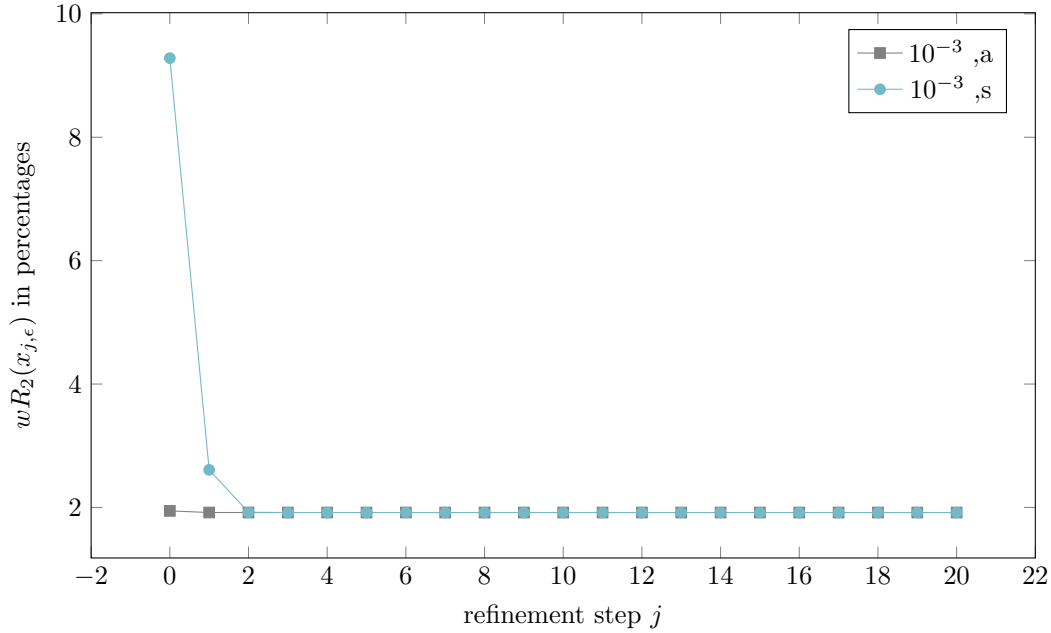

Figure S7: The progression of $wR_2(x_j)$ for $j = 0, 1, \ldots, 20$ and for $\delta = 10^{-3}$ Å, with label "a" for refinement journey starting from x_{appr} and label "s" starting from x_{spher} - all wR_2-factors are calculated with non-spherical form factors (ammonia)

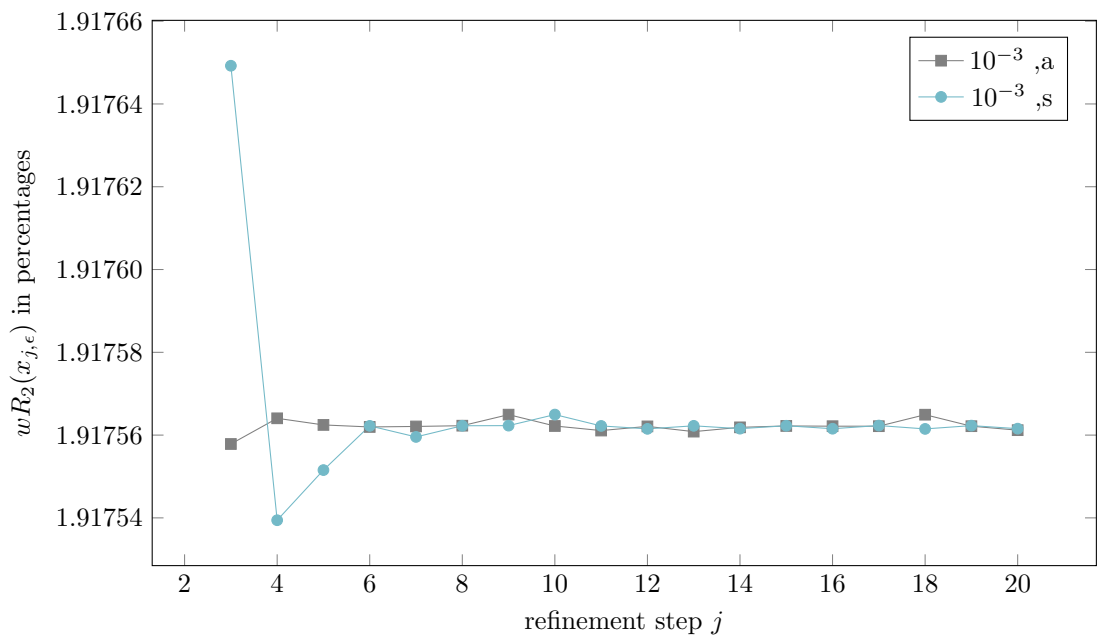

Figure S8: As in Figure S7; the progression of $wR_2(x_j)$ for $j = 3, 4, \ldots, 20$ and for $\delta = 10^{-3}$ Å, with label "a" for refinement journey starting from x_{appr} and label "s" starting from x_{spher} (ammonia)

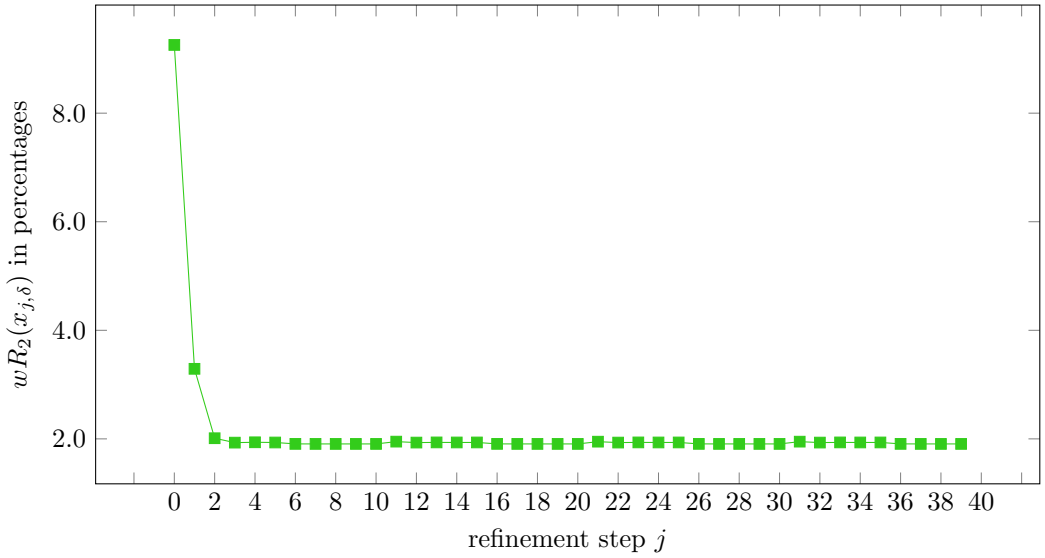

Figure S9: The progression of $wR_2(x_j)$ for $j = 0, 1, \ldots, 40$ and for $\delta = 10^{-3}$ Å starting from $\mathbf{x}_{\text{spher}}$ and alternating between 5 steps of approximate and numerical refinement (ammonia)

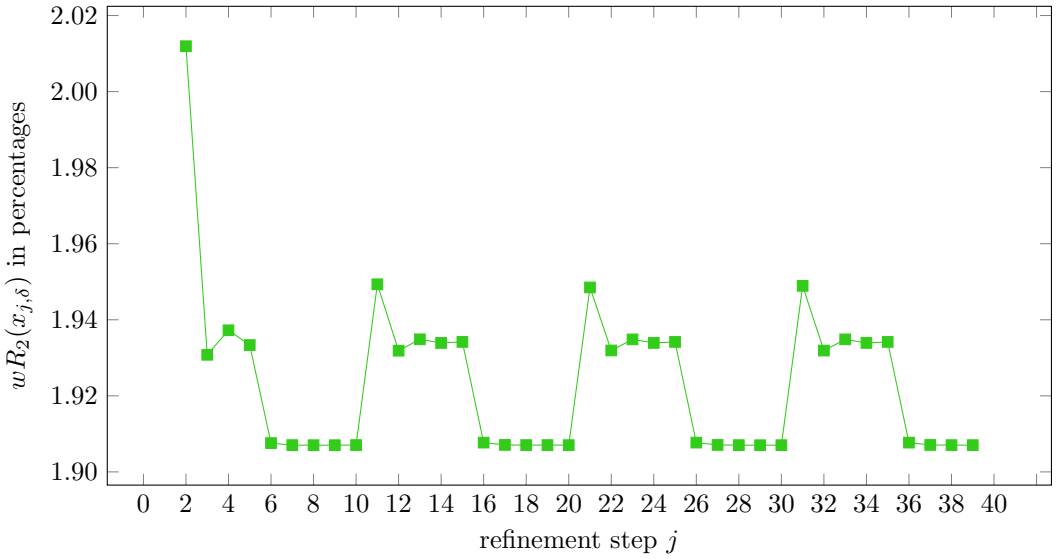

Figure S10: The progression of $wR_2(x_j)$ for $j = 2, 3, \ldots, 40$ and for $\delta = 10^{-3}$ Å starting from $\mathbf{x}_{\text{spher}}$ and alternating between 5 steps of approximate and numerical refinement (ammonia)

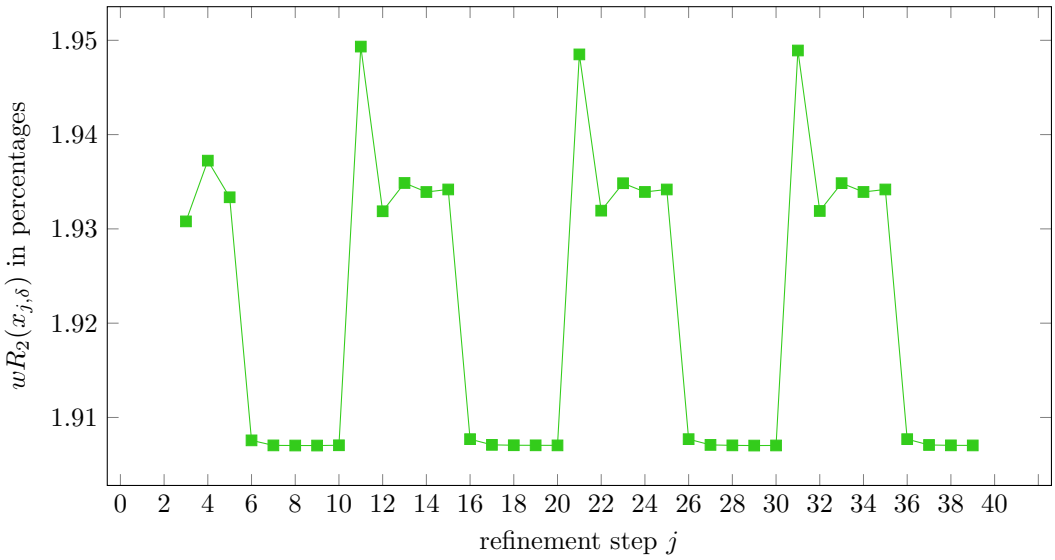

Figure S11: The progression of $wR_2(x_j)$ for $j = 3, 4, \ldots, 40$ and for $\delta = 10^{-3}$ Å and alternating between 5 steps of approximate and numerical refinement (ammonia)

3.3 wR2 diagrams (epoxide)

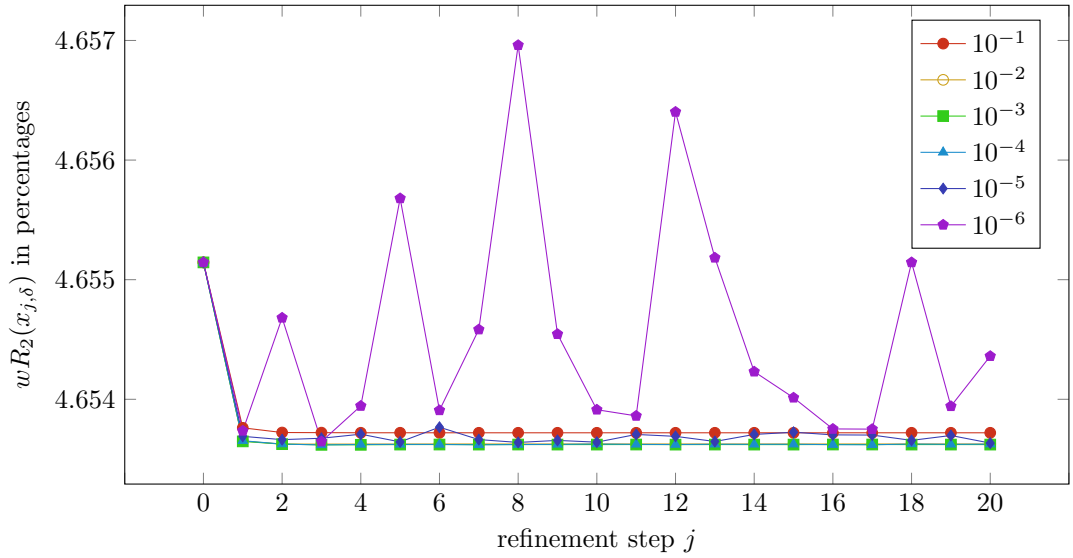

Figure S12: The progression of $wR_2(x_j)$ for $j = 0, 1, \ldots, 20$ and for $\delta = 10^{-1}, \ldots, 10^{-6}$ Å starting from $\mathbf{x}_{\text{appr}}$ (epoxide)

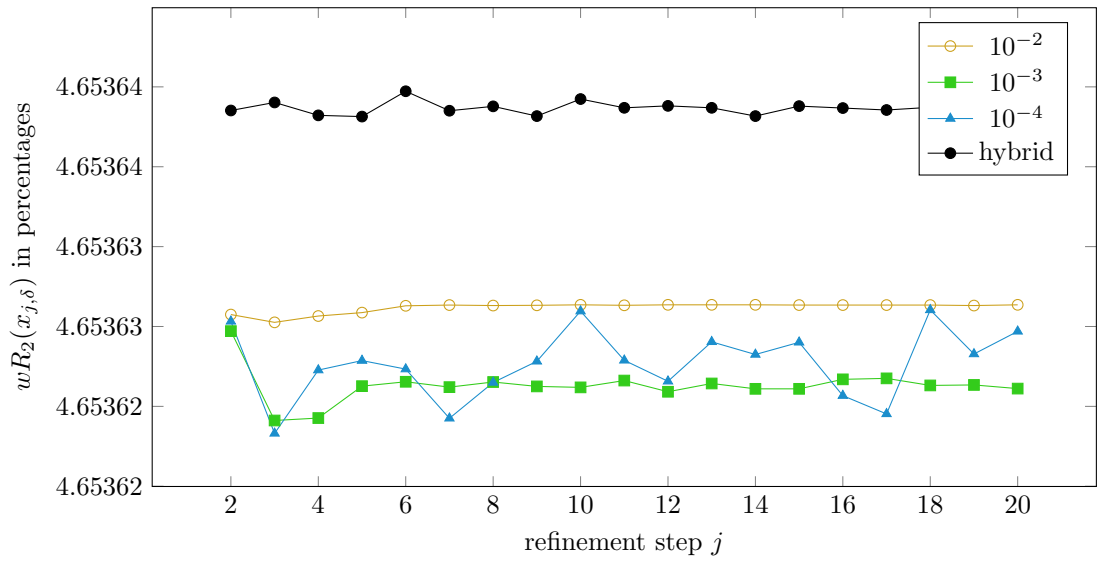

Figure S13: As in Figure S12 The progression of $wR_2(x_j)$ for $j = 2, 3, \ldots, 20$ and for $\delta = 10^{-2}$Å, 10^{-3}Å, 10^{-4}Å, and hybrid at $\delta = 10^{-3}$Å starting from $\mathbf{x}_{\text{appr}}$ (epoxide)

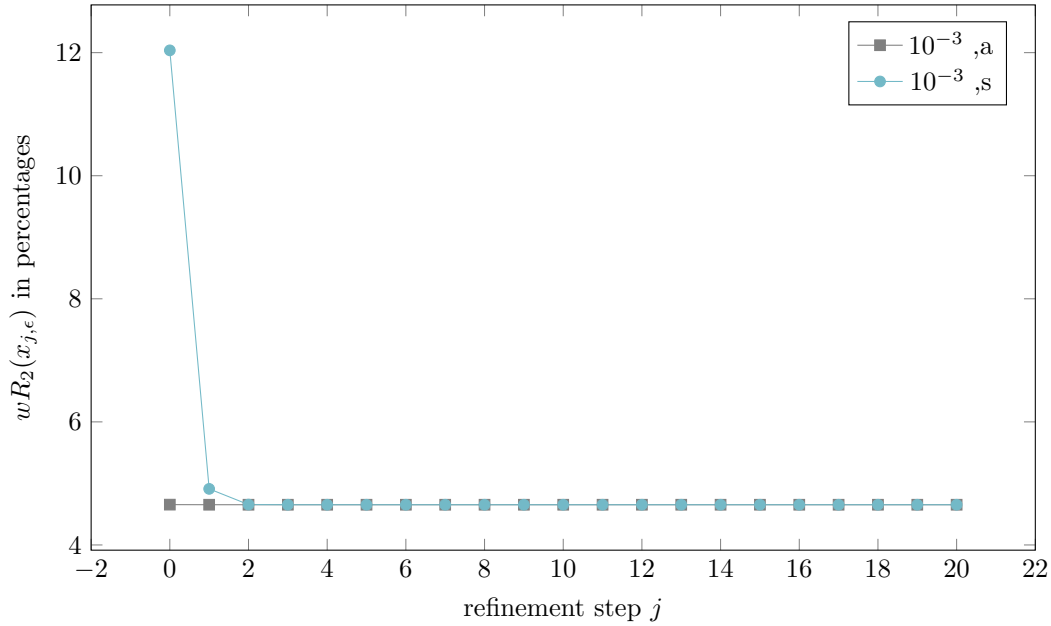

Figure S14: The progression of $wR_2(x_j)$ for $j = 0, 1, \ldots, 20$ and for $\delta = 10^{-3}$ Å, with label "a" for refinement journey starting from x_{appr} and label "s" starting from x_{spher} - all wR_2-factors are calculated with non-spherical form factors (epoxide)

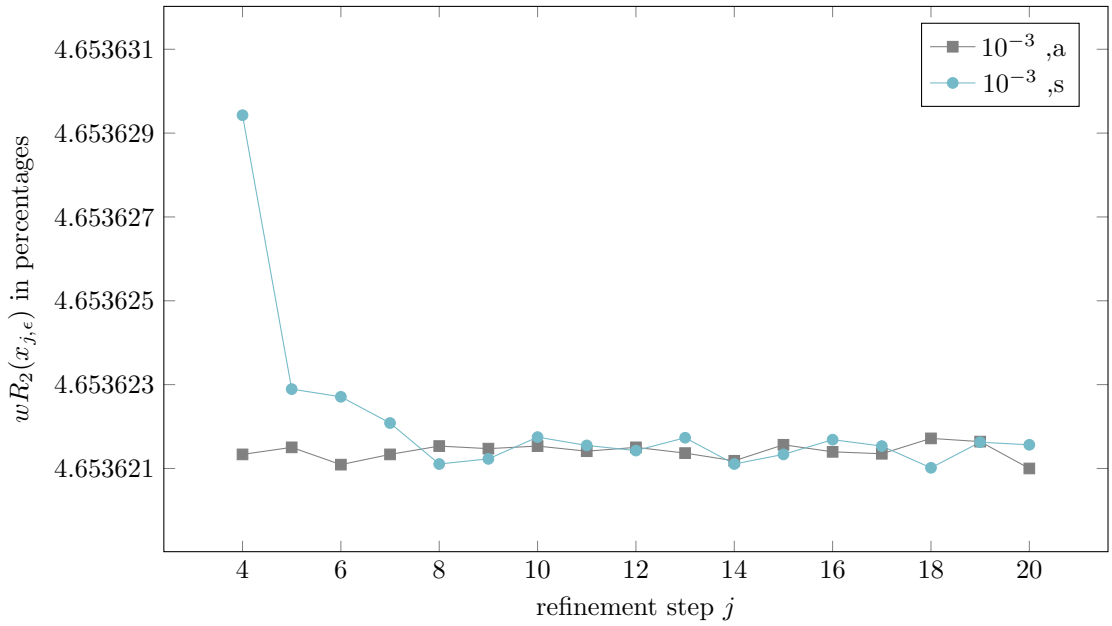

Figure S15: As in Figure S7; the progression of $wR_2(x_j)$ for $j = 4, 5, \ldots, 20$ and for $\delta = 10^{-3}$ Å, with label "a" for refinement journey starting from x_{appr} and label "s" starting from x_{spher} (epoxide)

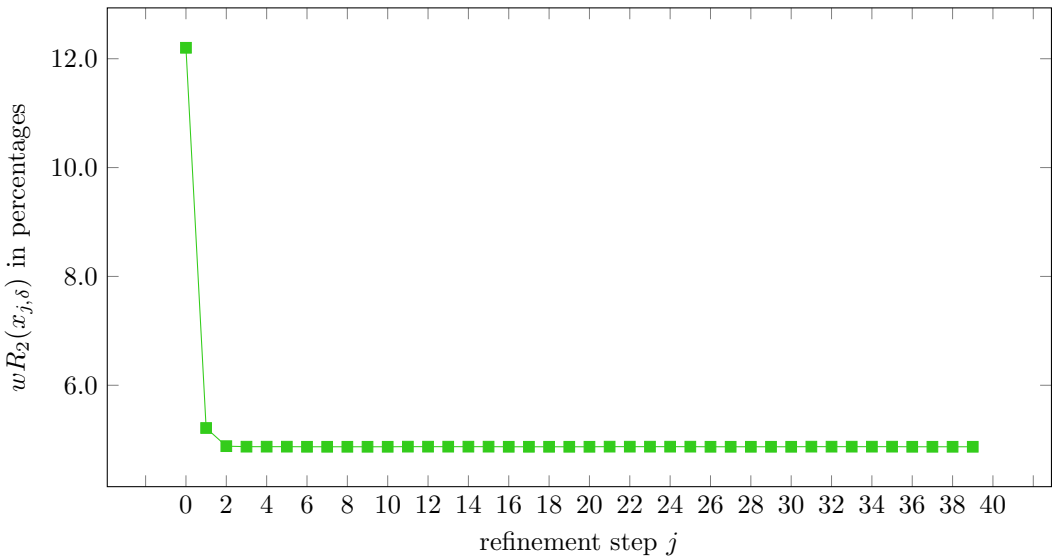

Figure S16: The progression of $wR_2(x_j)$ for $j = 0, 1, \ldots, 40$ and for $\delta = 10^{-3}$ Å and alternating between 5 steps of approximate and numerical refinement starting from $\mathbf{x}_{\text{spher}}$ (epoxide)

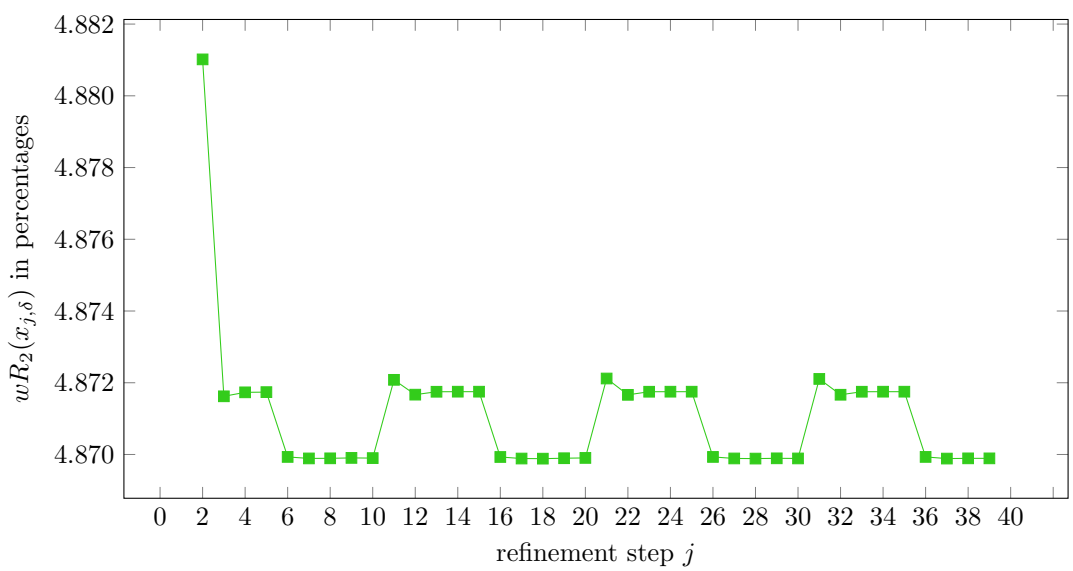

Figure S17: The progression of $wR_2(x_j)$ for $j = 2, 3, \ldots, 40$ and for $\delta = 10^{-3}$ Å and alternating between 5 steps of approximate and numerical refinement starting from $\mathbf{x}_{\text{spher}}$ (epoxide)

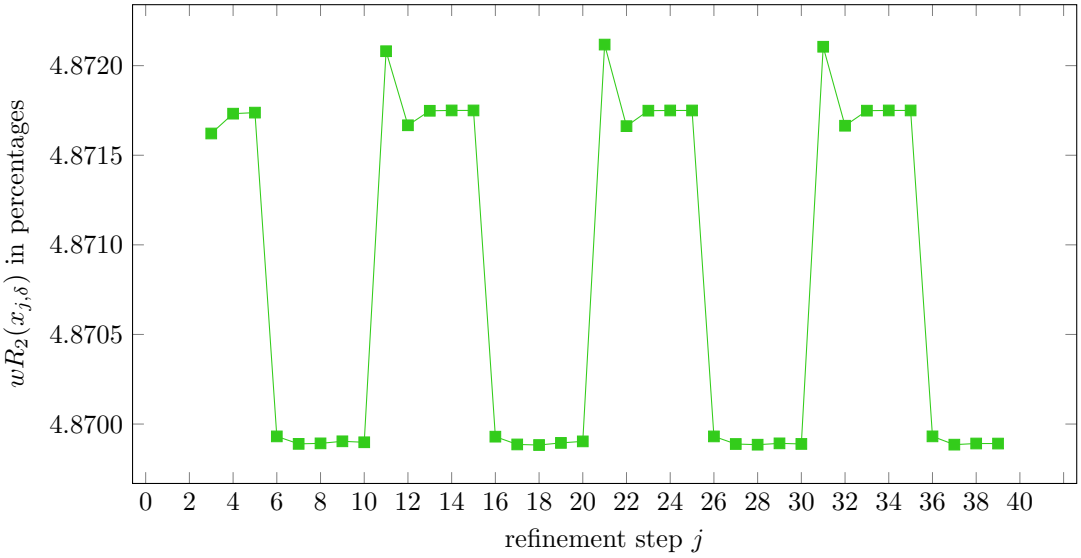

Figure S18: The progression of $wR_2(x_j)$ for $j = 3, 4, \ldots, 40$ and for $\delta = 10^{-3}$ Å and alternating between 5 steps of approximate and numerical refinement (epoxide)

3.4 wR2 diagrams (L-alanine)

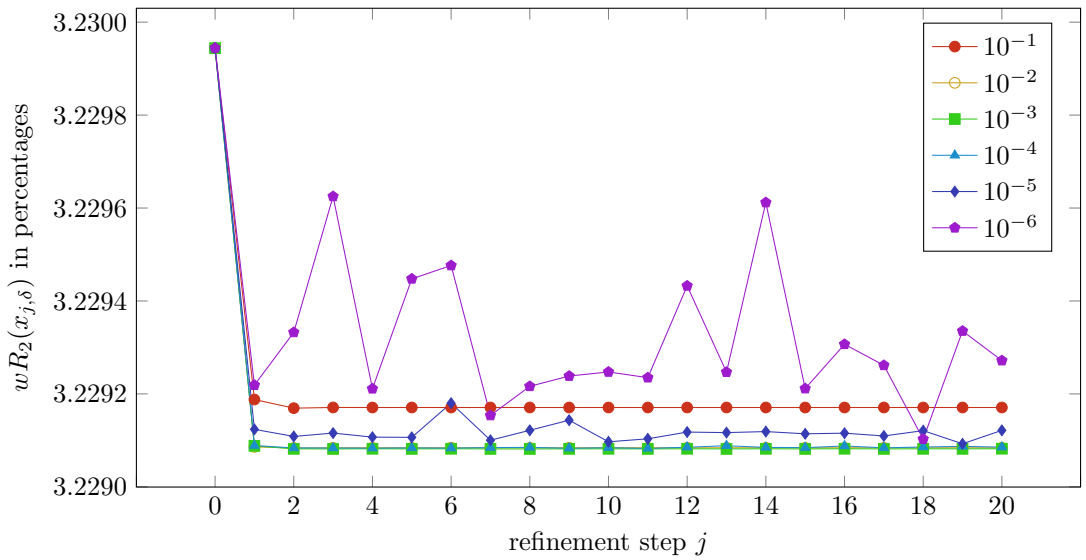

Figure S19: The progression of $wR_2(x_j)$ for $j = 0, 1, \ldots, 20$ and for $\delta = 10^{-1}, \ldots, 10^{-6}$Å starting from $\mathbf{x}_{\text{appr}}$ (L-alanine)

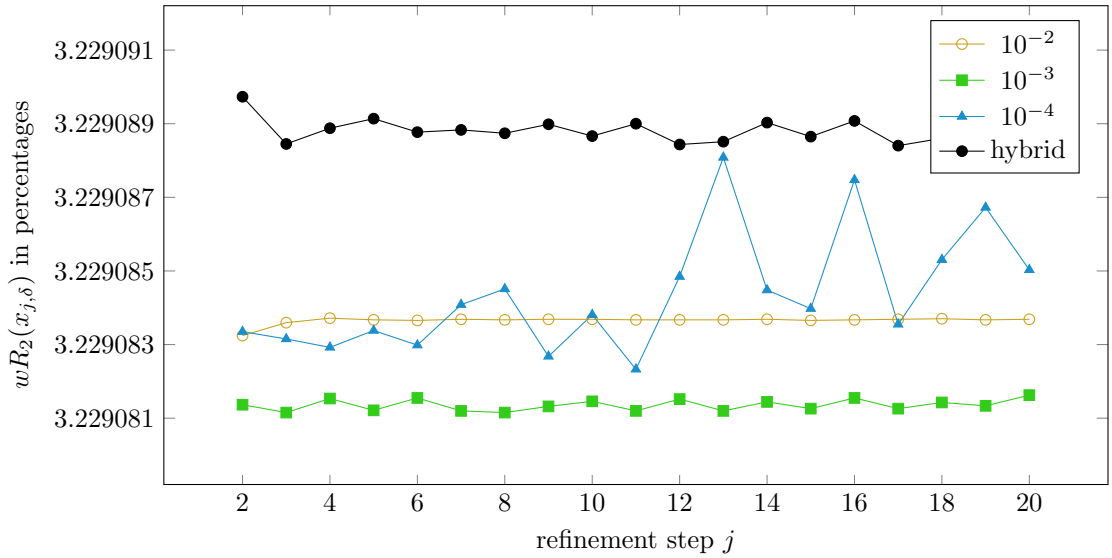

Figure S20: As in Figure S19; the progression of $wR_2(x_j)$ for $j = 2, 3, \ldots, 20$ and for $\delta = 10^{-2}$Å, 10^{-3}Å, 10^{-4}Å, and hybrid at $\delta = 10^{-3}$ starting from $\mathbf{x}_{\text{appr}}$ (L-alanine)

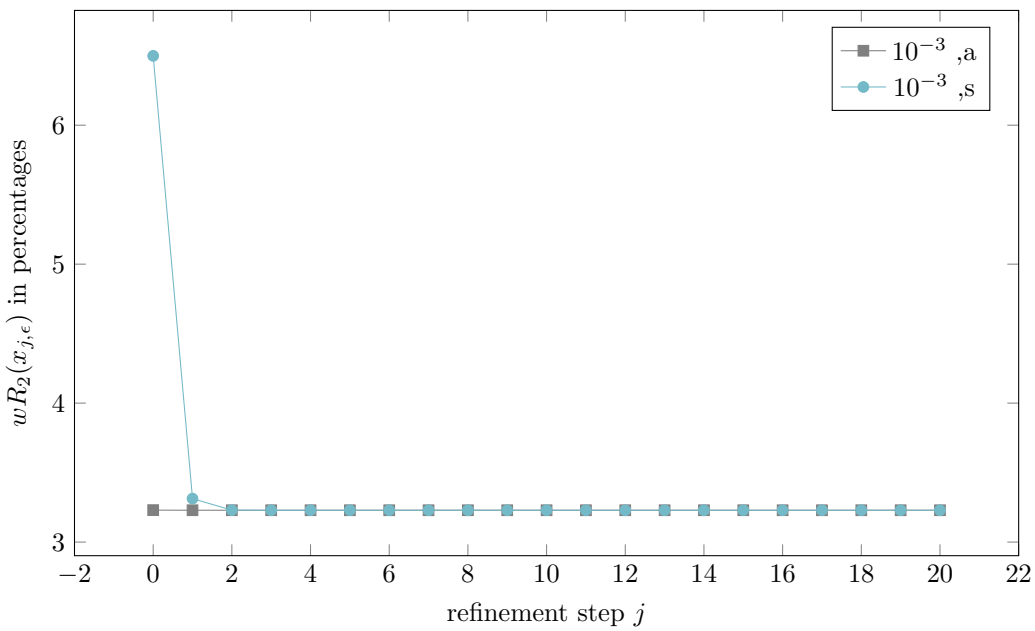

Figure S21: The progression of $wR_2(x_j)$ for $j = 0, 1, \ldots, 20$ and for $\delta = 10^{-3}$Å, with label "a" for refinement journey starting from x_{appr} and label "s" starting from x_{spher} - all wR_2-factors are calculated with non-spherical form factors (L-alanine)

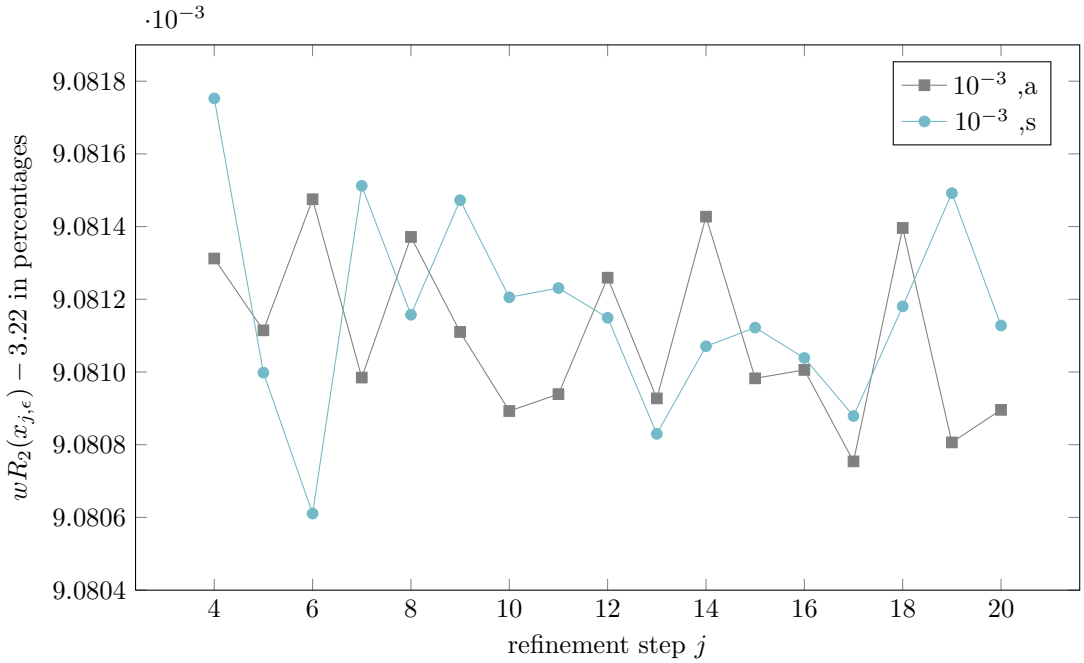

Figure S22: As in Figure S21; the progression of $wR_2(x_j) - 3.22$ for $j = 4, 5, \ldots, 20$ and for $\delta = 10^{-3}$Å, with label "a" for refinement journey starting from x_{appr} and label "s" starting from x_{spher} (L-alanine)

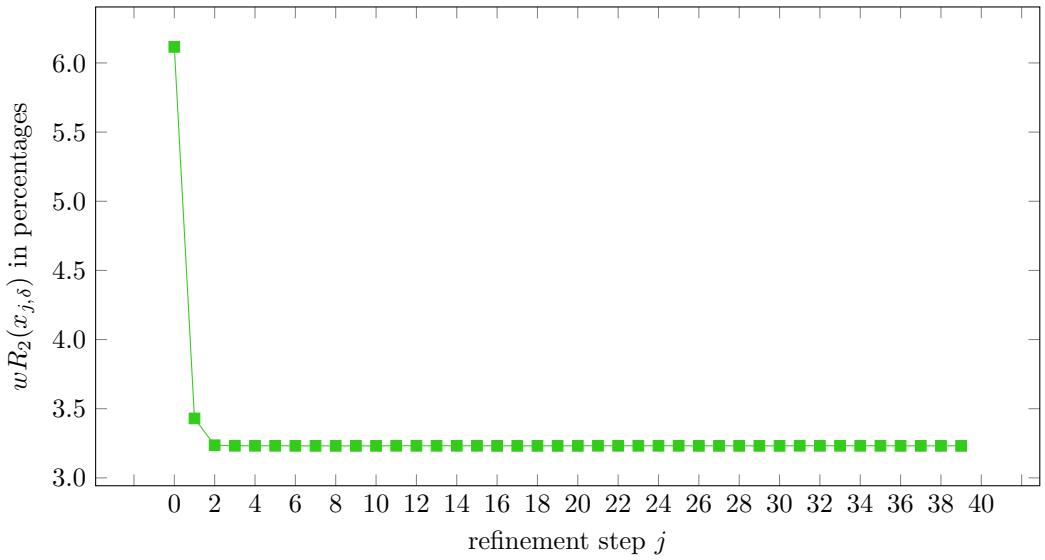

Figure S23: The progression of $wR_2(x_j)$ for $j = 0, 1, \ldots, 40$ and for $\delta = 10^{-3}$ Å and alternating between 5 steps of approximate and numerical refinement starting from $\mathbf{x}_{\text{spher}}$ (L-alanine)

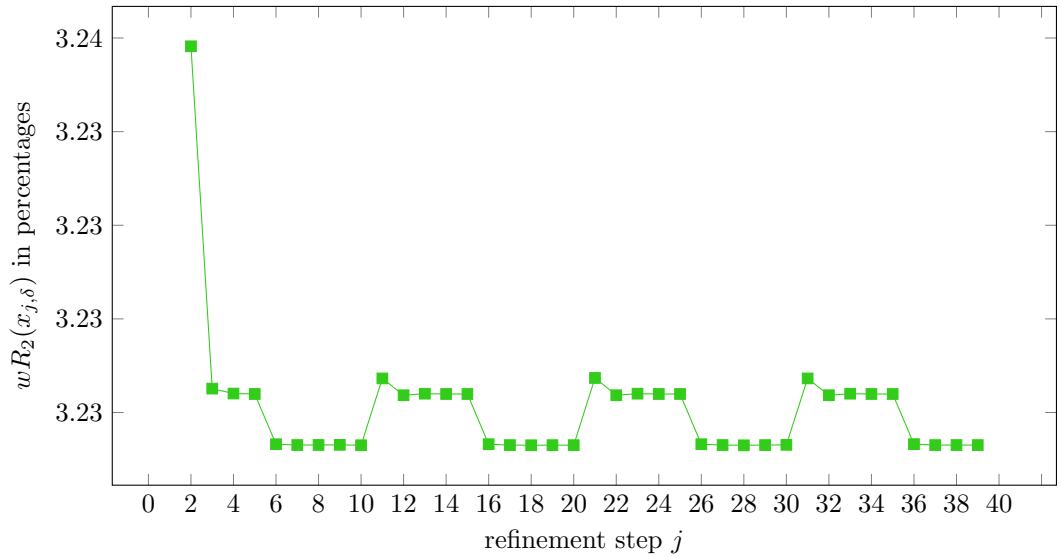

Figure S24: The progression of $wR_2(x_j)$ for $j = 2, 3, \ldots, 40$ and for $\delta = 10^{-3}$ Å and alternating between 5 steps of approximate and numerical refinement starting from $\mathbf{x}_{\text{spher}}$ (L-alanine)

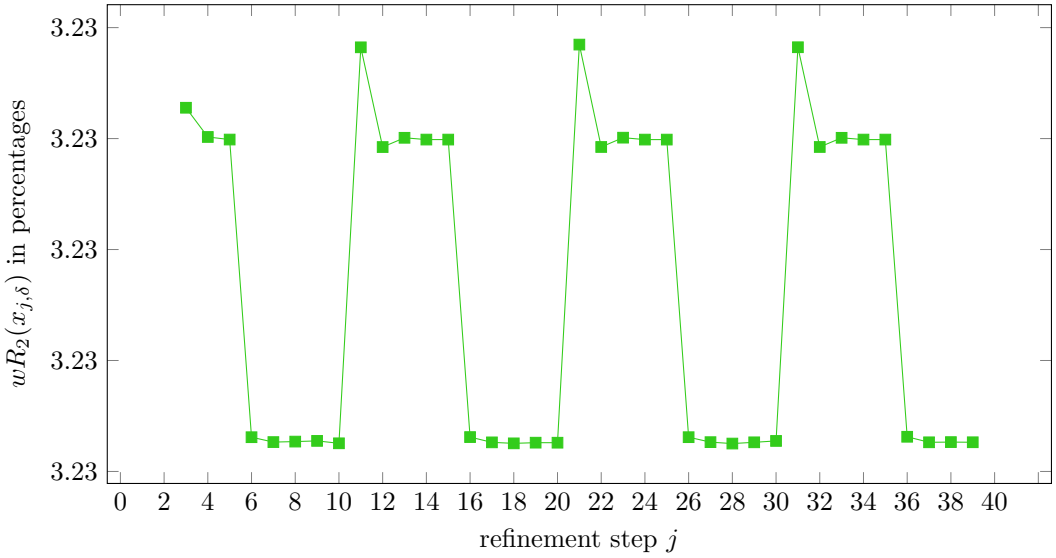

Figure S25: The progression of $wR_2(x_j)$ for $j = 3, 4, \ldots, 40$ and for $\delta = 10^{-3}$ Å and alternating between 5 steps of approximate and numerical refinement (L-alanine)

3.5 L-Alanine by TAAM

Here we present the equivalent of Figures 5 and 6 for numerical non-spherical refinement of L-Alanine utilising DISCAMB rather than ORCA. The improvement from this refinement is smaller and more reliant on the correct choice of δ, but nevertheless provides proof of the principle of numerical refinement beyond ORCA - both of the improvement that may be gained by correctly modelling these derivatives, and of the already present high accuracy of approximate non-spherical refinement.

Figure S26 shows the shift/esd for numerical refinement on L-Alanine via DISCAMB. In this case, 10^{-3} joins the other smaller δ as an unviable choice, but $\delta = 10^{-1}$ and 10^{-2} remain viable.

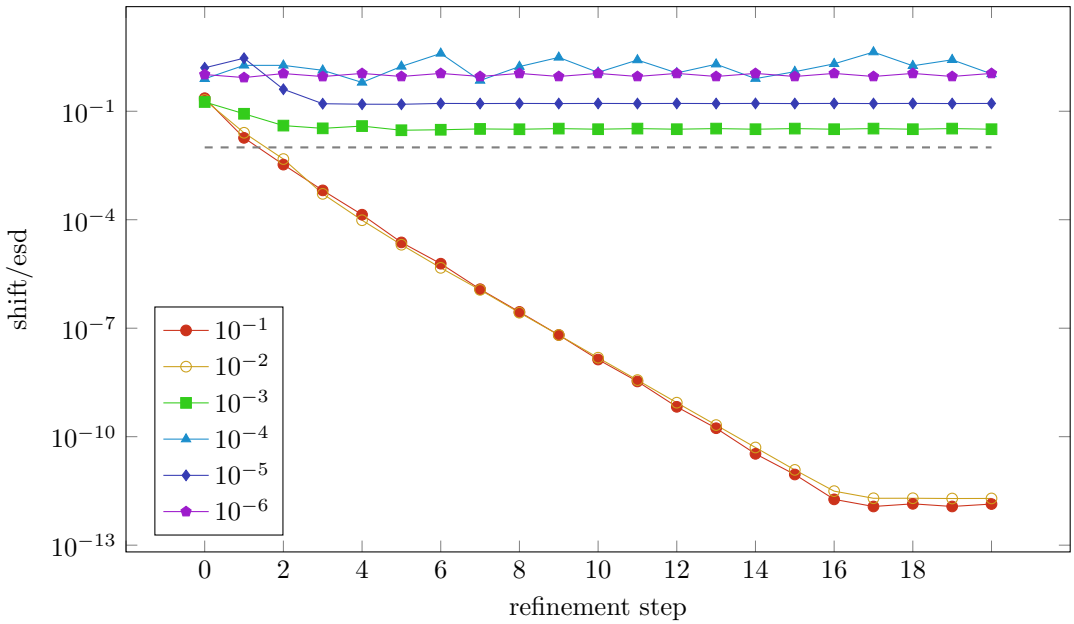

Figure S26: Maximal shift/esd for numerical refinement starting from $\mathbf{x}_{\text{appr}}$ for $\delta = 10^{-1}$, ..., 10^{-6}Å, (L-alanine via DISCAMB)

Figure S27 presents the progression of wR_2 for these tested δ, but the instability of $\delta = 10^{-4}, 10^{-5}$ and 10^{-6} prevents this diagram from presenting useful information. We look to S28 which shows that $\delta = 10^{-2}$ and 10^{-3} provide the required drop to wR_2, and as $\delta = 10^{-2}$ satisfies both, we find that our method remains effective.

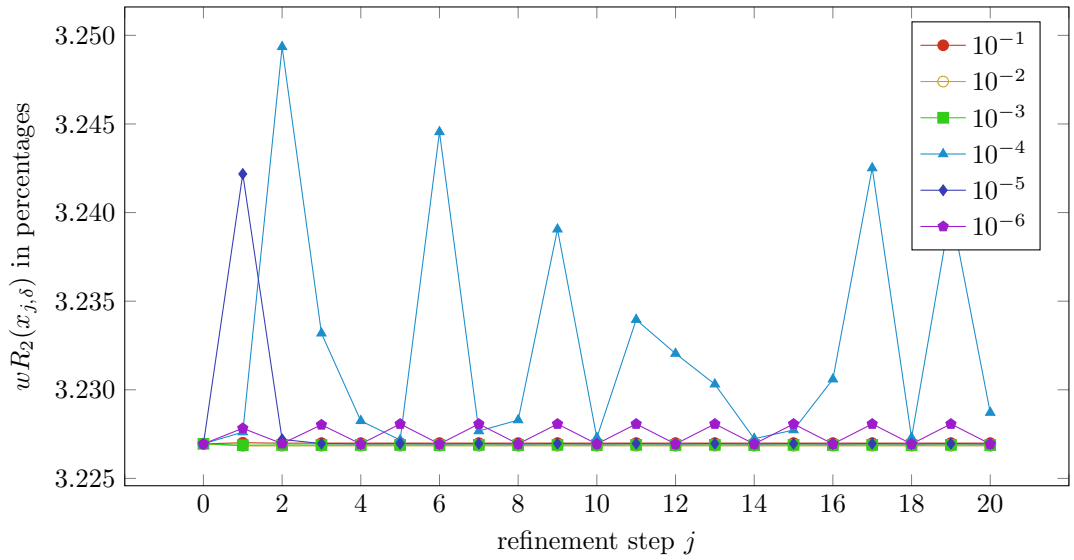

Figure S27: The progression of $wR_2(x_j)$ for $j = 0, 1, \ldots, 20$ and for $\delta = 10^{-1}, \ldots, 10^{-6}$Å starting from $\mathbf{x}_{\text{appr}}$ (L-alanine via DISCAMB)

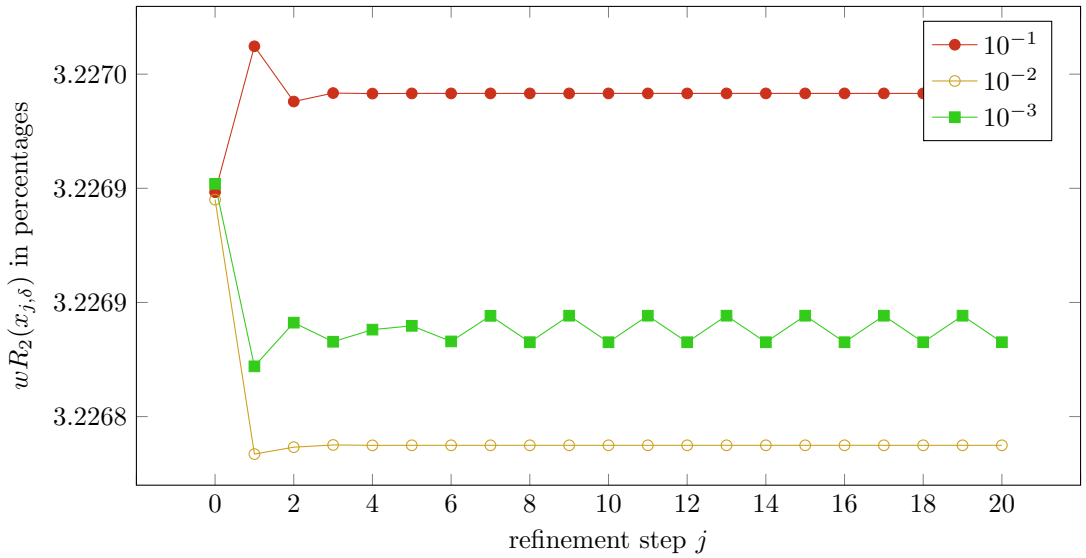

Figure S28: As in Figure S19; the progression of $wR_2(x_j)$ for $j = 0, 1, \ldots, 20$ and for $\delta = 10^{-1}$Å, 10^{-2}Å, 10^{-3}Å, starting from $\mathbf{x}_{\text{appr}}$ (L-alanine via DISCAMB)

3.6 Table 2

We present an extended version of Table 2 of the main article. This contains details of which atom attains the largest difference between the two refinements (shown in brackets in each applicable column), as well as columns showing the largest Cartesian atomic shift. This confirms our statements that the difference between the two refinements (starting from $\mathbf{x}_{\text{spher}}$ and $\mathbf{x}_{\text{appr}}$) are about the same size as the maximal Cartesian shifts of the individual atoms from the model $\mathbf{x}_k$ to the model $\mathbf{x}_{k+1}$, from the 7th step onward.

step	shift/esd ($\times 10^5$) (from $\mathbf{x}_{\text{spher}}$)	shift/esd ($\times 10^5$) (from $\mathbf{x}_{\text{appr}}$)	wR_2 (from $\mathbf{x}_{\text{spher}}$)	wR_2 (from $\mathbf{x}_{\text{appr}}$)	maximal atomic distance (in 10^{-6}Å)	maximal Cartesian atomic shift (in 10^{-6}Å) (from $\mathbf{x}_{\text{spher}}$)	maximal Cartesian atomic shift (in 10^{-6}Å) (from $\mathbf{x}_{\text{appr}}$)
Ammonia							
k=0	392693	143955	9.2821%	1.9440%	126974(H)	-	-
k=1	198189	18797	2.6092%	1.9180%	20665(H)	115659(H)	9355(H)
k=2	47387	2818	1.9216%	1.9176%	2458(H)	21309(H)	981(H)
k=3	7724	760	1.9176%	1.9176%	380(H)	2457(H)	168(H)
k=4	1823	324	1.9175%	1.9176%	102(H)	420(H)	44(H)
k=5	592	142	1.9176%	1.9176%	36(H)	127(H)	15(H)
k=6	140	78	1.9176%	1.9176%	11(H)	35(H)	7(H)
k=7...20	$\leq$88	$\leq$119	1.9176%	1.9176%	$\leq$5(H)	$\leq$8(H)	$\leq$6(H)
Epoxide							
k=0	674626	51117	12.0375%	4.6551%	130527(H3a)	-	-
k=1	281762	4568	4.9113%	4.6536%	21095(H2b)	124253(H3a)	4694(H3a)
k=2	35810	812	4.6561%	4.6536%	3093(H3a)	21697(H3b)	321(H3a)
k=3	6868	476	4.6537%	4.6536%	461(H3b)	2653(H3a)	80(H3a)
k=4	1365	152	4.6536%	4.6536%	136(H3a)	458(H3b)	45(H3a)
k=5	292	88	4.6536%	4.6536%	38(H3a)	93(H3a)	12(H2b)
k=6	138	102	4.6536%	4.6536%	16(H3b)	27(H3a)	9(H3b)
k=7...20	$\leq$99	$\leq$126	4.6536%	4.6536%	$\leq$11(H3b)	$\leq$12(H3a)	$\leq$13(H3b)
L-Alanine							
k=0	992154	50245	6.4989%	3.2299%	126479(H2b)	-	-
k=1	308603	3568	3.3127%	3.2291%	24140(H1a)	110776(H2b)	4802(H1c)
k=2	32231	641	3.2298%	3.2291%	1818(H1a)	22253(H1a)	172(H1a)
k=3	7711	244	3.2291%	3.2291%	237(H1c)	1655(H1a)	18(H1b)
k=4	1838	176	3.2291%	3.2291%	59(H1b)	194(H1c)	19(H1b)
k=5	431	202	3.2291%	3.2291%	20(H1b)	50(H1b)	13(H1c)
k=6	214	194	3.2291%	3.2291%	16(H1b)	16(H1b)	14(H1c)
k=7...20	$\leq$190	$\leq$267	3.2291%	3.2291%	$\leq$14(H1a)	$\leq$19(H1b)	$\leq$14(H1a)

Table S2: Progression of refinement values from $\mathbf{x}_{\text{spher}}$ and $\mathbf{x}_{\text{appr}}$ via numerical nonspherical refinement with $\delta = 10^{-3}$Å. In the first two columns, if the shift/esd is below 0.01, it is colored green, else red. The 3rd last column represents the maximal distance between sites of corresponding atoms through numerical nonspherical refinement from these two start points, whilst the last two columns represent the maximal Cartesian atomic shift within the given refinement path.

4 Comparison of refinement minima

4.1 Basis set dependence

The following Figures S29 and S30 add in the 'High' integration grid (shown as a lightened colour) and the 'Low' integration grid (shown as a darkened colour) to Figure 8 from the main paper. It is clear that the impact of these is minimal compared to the other differences

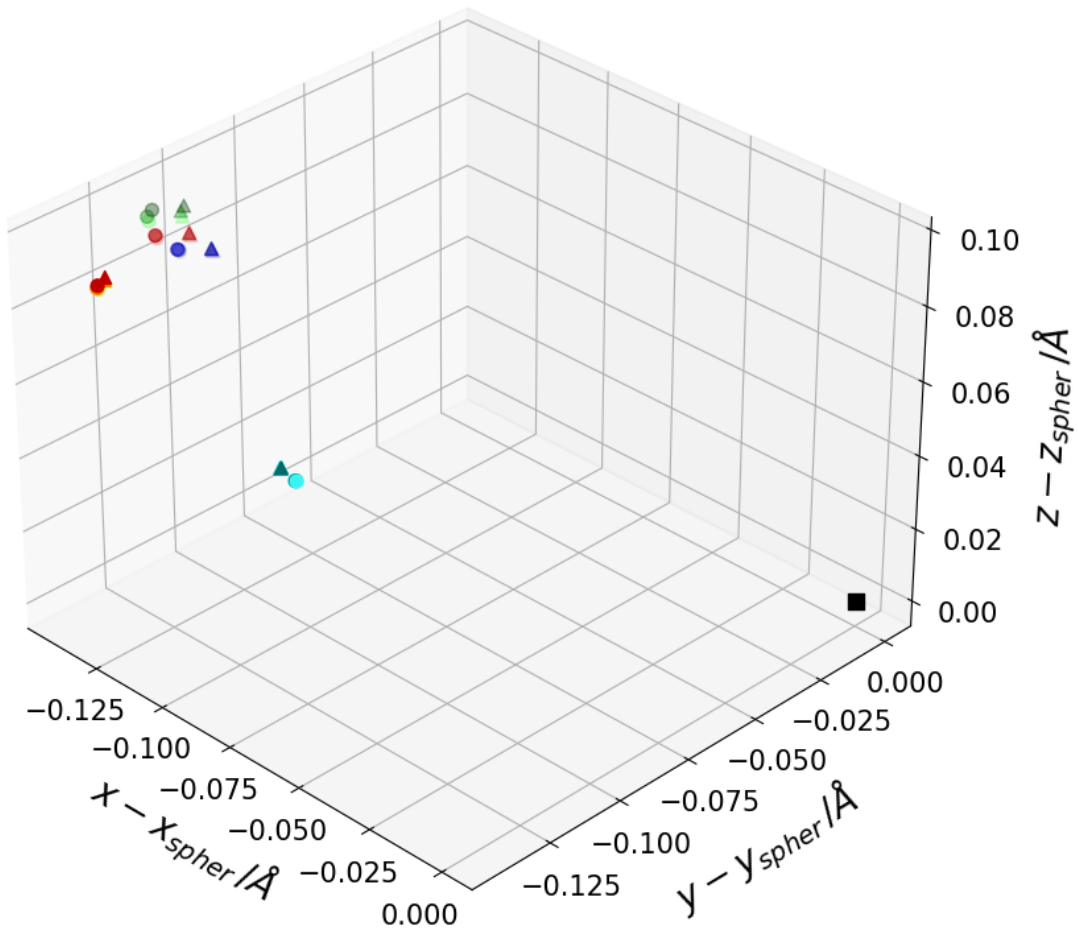

Figure S29: The position of the hydrogen atom (in Å) at the final model, obtained through classical spherical refinement (■) and non-spherical refinement processes (approximate ▲ and numerical ●) using various basis sets, where the hydrogen atom in the classical spherical model is shifted to the origin (0,0,0).
The colours are as follows: cc-pVQZ (top), cc-pVTZ (second-top), def2-TZVP (third top), 3-21G (lower cluster), def2-SVP (left cluster), with darkened and lightened versions of these colours corresponding to 'low' or 'high' rather than 'normal' integration accuracy, respectively. (ammonia)

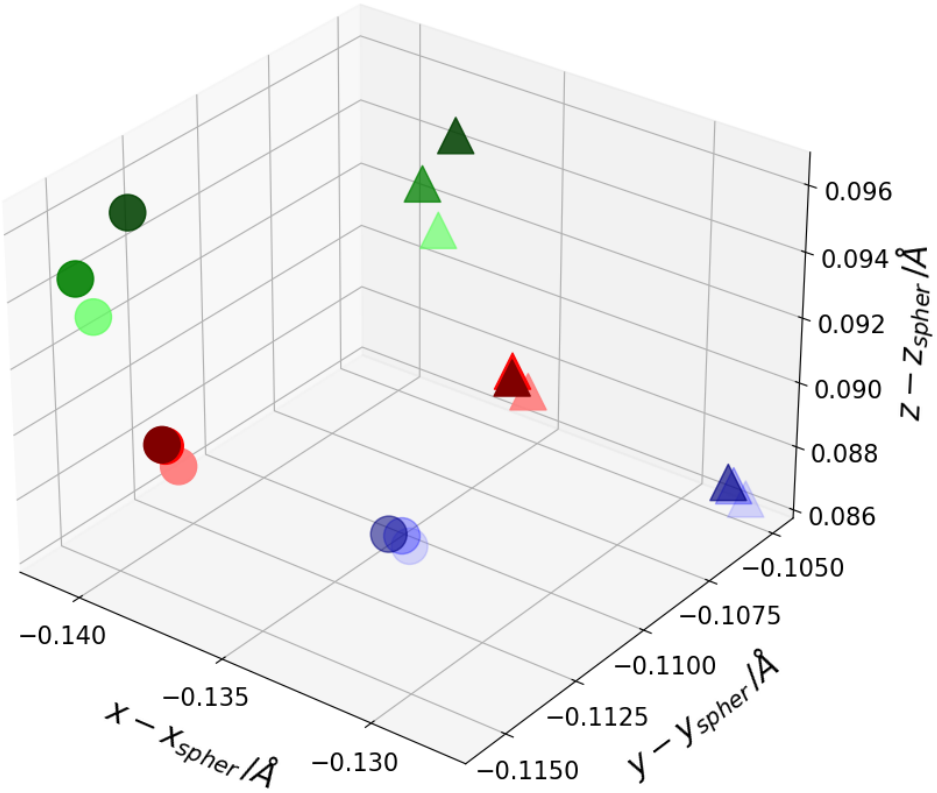

Figure S30: A small area of Figure S29: The position of the hydrogen atom at the final model, obtained with the larger three basis sets, cc-pVQZ (top), cc-pVTZ (middle), def2-TZVP (bottom), relative to the position of the hydrogen in the classical spherical model (which would appear at (0,0,0)). (ammonia)

5 Bringing In Uncertainties

We present the uncertainty ball diagrams for all atoms of our three molecules, with diagrams comparing the ADPs in a matching fashion. Tables providing the uncertainty radii are presented alongside the relevant diagrams. In all cases, the white dot represents the numerical nonspherical refinement's final model, the black dot represents the approximate nonspherical refinement's final model, the red dot represents the spherical final model.

5.1 Ammonia

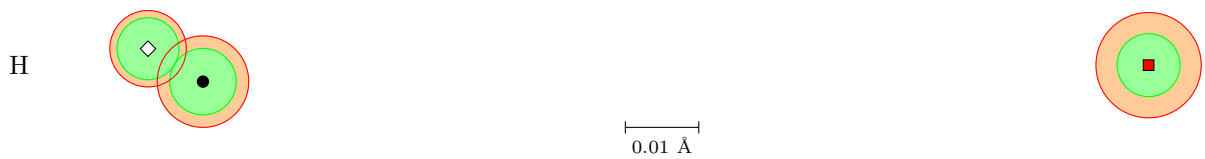

Figure S31: Positions of the hydrogen atoms in $\mathbf{x}_{\text{num}}$ (white ⋄), $\mathbf{x}_{\text{appr}}$ (black ●) and $\mathbf{x}_{\text{spher}}$ (red ■), and their uncertainty balls. Green balls represent inner uncertainty balls and red balls represent outer uncertainty balls. (ammonia)

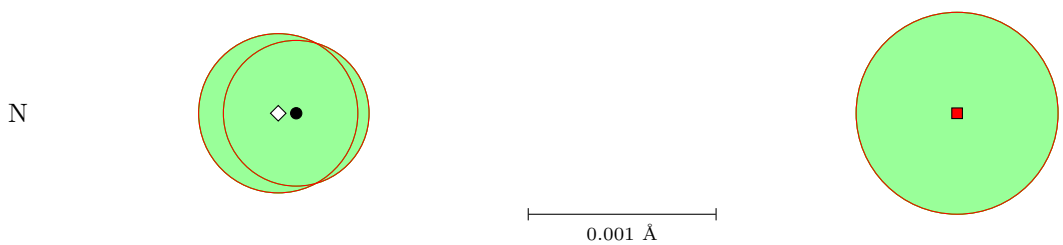

Figure S32: Positions of the non-hydrogen atoms in $\mathbf{x}_{\text{num}}$ (white ⋄), $\mathbf{x}_{\text{appr}}$ (black ●) and $\mathbf{x}_{\text{spher}}$ (red ■), and their uncertainty balls. Green balls represent inner uncertainty balls and red balls represent outer uncertainty balls. (ammonia)

	$\lVert A_{\text{num}} - A_{\text{spher}} \rVert$	$r(A_{\text{num}})$	$R(A_{\text{num}})$	$r(A_{\text{spher}})$	$R(A_{\text{spher}})$
A=N	3.592e-03	4.214e-04	4.214e-04	5.344e-04	5.344e-04
A=H	1.343e-01	4.160e-03	5.131e-03	4.225e-03	7.067e-03
	$\lVert A_{\text{num}} - A_{\text{appr}} \rVert$	$r(A_{\text{num}})$	$R(A_{\text{num}})$	$r(A_{\text{appr}})$	$R(A_{\text{appr}})$
A=N	9.513e-05	4.214e-04	4.214e-04	3.856e-04	3.856e-04
A=H	8.598e-03	4.160e-03	5.131e-03	4.468e-03	6.141e-03

Table S3: Positional difference (in Å) between atoms in $\mathbf{x}_{\text{num}}$, $\mathbf{x}_{\text{appr}}$, and $\mathbf{x}_{\text{spher}}$ and their comparison with uncertainty bounds. Red indicates a bound smaller than the difference, whilst green represents a bound larger than the difference (ammonia).

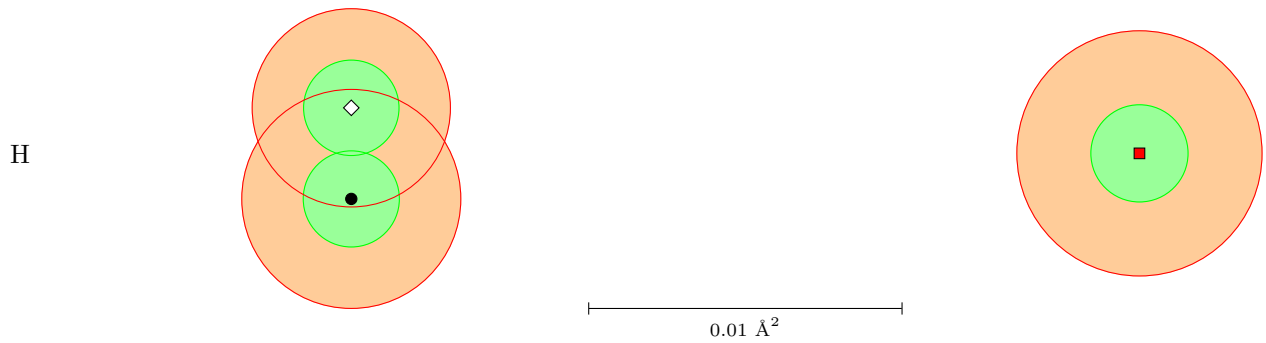

Figure S33: ADPs of the hydrogen atoms in $\mathbf{x}_{\mathrm{num}}$ (white ◇), $\mathbf{x}_{\mathrm{appr}}$ (black ●) and $\mathbf{x}_{\mathrm{spher}}$ (red ■), and their uncertainty balls. Green balls represent inner uncertainty balls and red balls represent outer uncertainty balls. (ammonia)

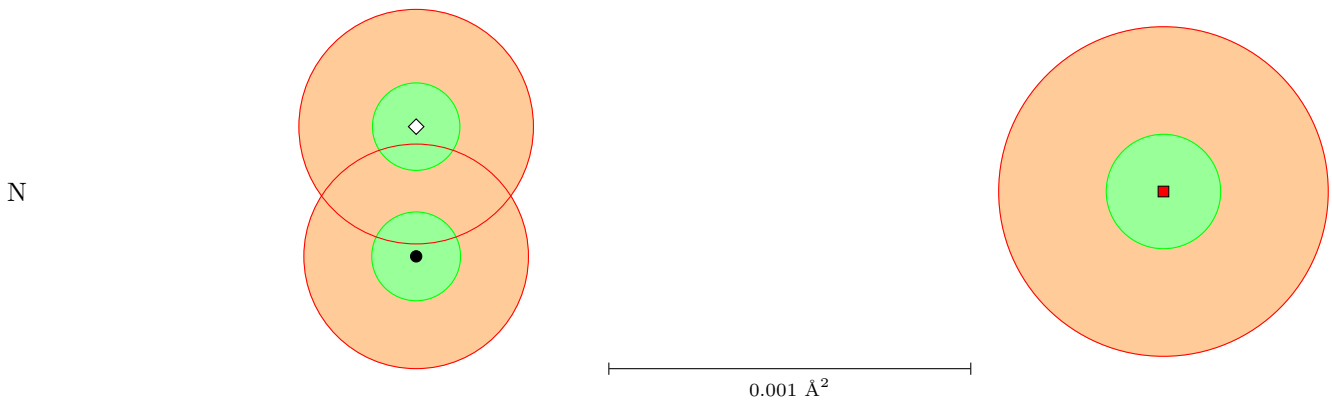

Figure S34: ADPs of the non-hydrogen atoms in $\mathbf{x}_{\mathrm{num}}$ (white ◇), $\mathbf{x}_{\mathrm{appr}}$ (black ●) and $\mathbf{x}_{\mathrm{spher}}$ (red ■), and their uncertainty balls. Green balls represent inner uncertainty balls and red balls represent outer uncertainty balls. (ammonia)

	$\|A_{\text{num}} - A_{\text{spher}}\|$	$r(A_{\text{num}})$	$R(A_{\text{num}})$	$r(A_{\text{spher}})$	$R(A_{\text{spher}})$
A=N	1.972e-03	1.205e-04	3.230e-04	1.576e-04	4.539e-04
A=H	2.536e-02	1.517e-03	3.153e-03	1.546e-03	3.899e-03
	$\|A_{\text{num}} - A_{\text{appr}}\|$	$r(A_{\text{num}})$	$R(A_{\text{num}})$	$r(A_{\text{appr}})$	$R(A_{\text{appr}})$
A=N	3.572e-04	1.205e-04	3.230e-04	1.223e-04	3.093e-04
A=H	2.896e-03	1.517e-03	3.153e-03	1.529e-03	3.483e-03

Table S4: ADP difference (in Å^2) between atoms in $\mathbf{x}_{\text{num}}$, $\mathbf{x}_{\text{appr}}$, and $\mathbf{x}_{\text{spher}}$ and their comparison with uncertainty bounds. Red indicates a bound smaller than the difference, whilst green represents a bound larger than the difference (ammonia).

5.2 Epoxide

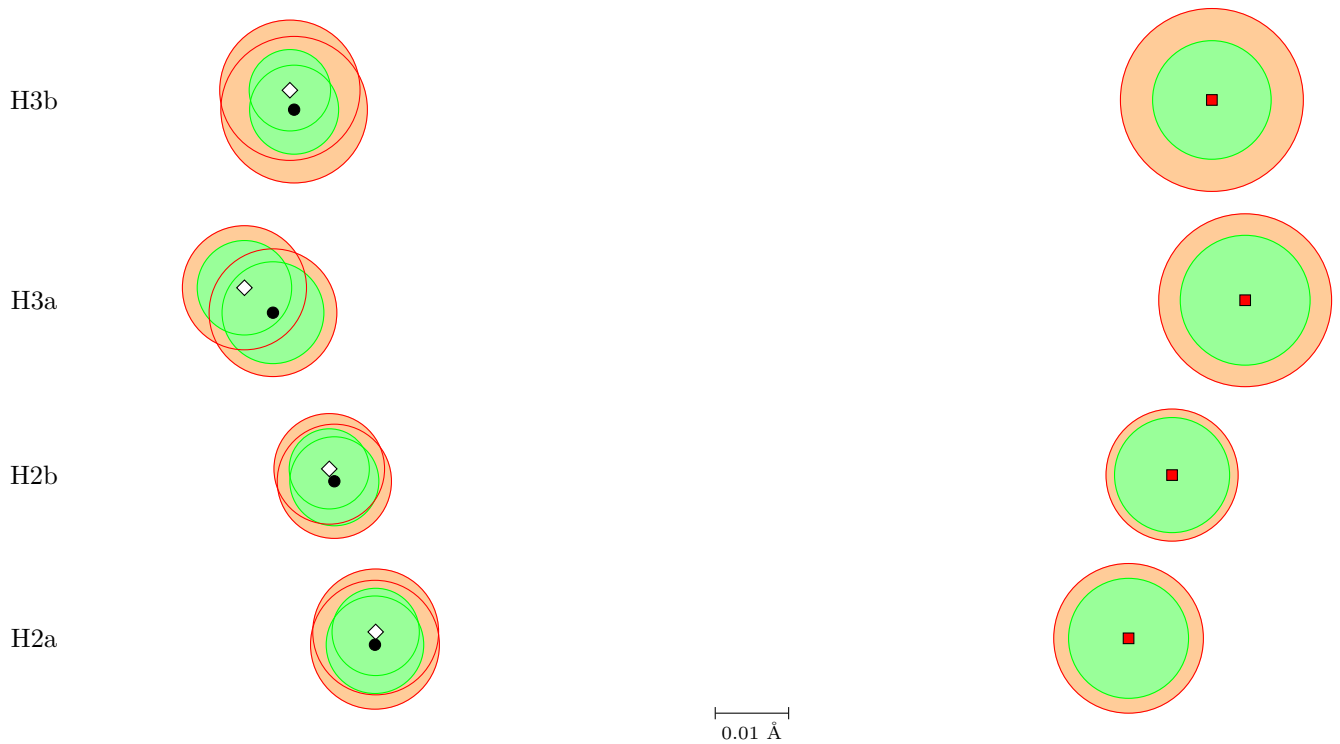

Figure S35: Positions of the hydrogen atoms in $\mathbf{x}_{\text{num}}$ (white ◇), $\mathbf{x}_{\text{appr}}$ (black ●) and $\mathbf{x}_{\text{spher}}$ (red ■), and their uncertainty balls. Green balls represent inner uncertainty balls and red balls represent outer uncertainty balls. (epoxide)

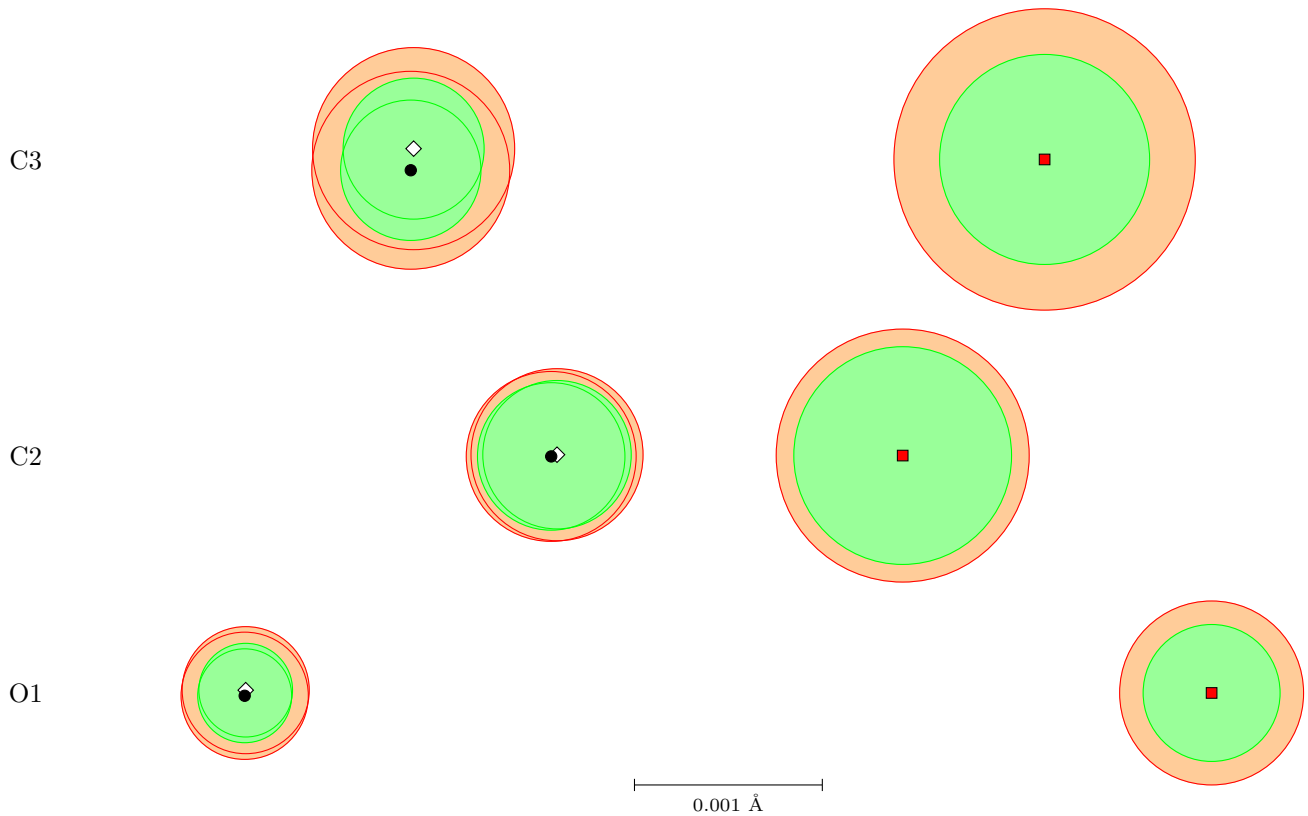

Figure S36: Positions of the non-hydrogen atoms in $\mathbf{x}_{\text{num}}$ (white ⋄), $\mathbf{x}_{\text{appr}}$ (black ●) and $\mathbf{x}_{\text{spher}}$ (red ■), and their uncertainty balls. Green balls represent inner uncertainty balls and red balls represent outer uncertainty balls. (epoxide)

	$\lVert A_{\text{num}} - A_{\text{spher}} \rVert$	$r(A_{\text{num}})$	$R(A_{\text{num}})$	$r(A_{\text{spher}})$	$R(A_{\text{spher}})$
A=O1	5.112e-03	2.479e-04	3.363e-04	3.624e-04	4.868e-04
A=C2	1.829e-03	3.928e-04	4.554e-04	5.763e-04	6.695e-04
A=H2a	1.011e-01	5.859e-03	8.449e-03	8.055e-03	1.005e-02
A=H2b	1.131e-01	5.380e-03	7.425e-03	7.726e-03	8.868e-03
A=C3	3.340e-03	3.731e-04	5.349e-04	5.559e-04	7.975e-04
A=H3a	1.344e-01	6.341e-03	8.333e-03	8.716e-03	1.160e-02
A=H3b	1.238e-01	5.464e-03	9.420e-03	7.960e-03	1.228e-02
	$\lVert A_{\text{num}} - A_{\text{appr}} \rVert$	$r(A_{\text{num}})$	$R(A_{\text{num}})$	$r(A_{\text{appr}})$	$R(A_{\text{appr}})$
A=O1	3.014e-05	2.479e-04	3.363e-04	2.485e-04	3.368e-04
A=C2	3.207e-05	3.928e-04	4.554e-04	3.903e-04	4.497e-04
A=H2a	1.722e-03	5.859e-03	8.449e-03	6.546e-03	8.652e-03
A=H2b	1.799e-03	5.380e-03	7.425e-03	5.975e-03	7.668e-03
A=C3	1.154e-04	3.731e-04	5.349e-04	3.715e-04	5.238e-04
A=H3a	5.085e-03	6.341e-03	8.333e-03	6.837e-03	8.576e-03
A=H3b	2.668e-03	5.464e-03	9.420e-03	5.976e-03	9.838e-03

Table S5: Positional difference (in Å) between atoms in $\mathbf{x}_{\text{num}}$, $\mathbf{x}_{\text{appr}}$, and $\mathbf{x}_{\text{spher}}$ and their comparison with uncertainty bounds. Red indicates a bound smaller than the difference, whilst green represents a bound larger than the difference (epoxide).

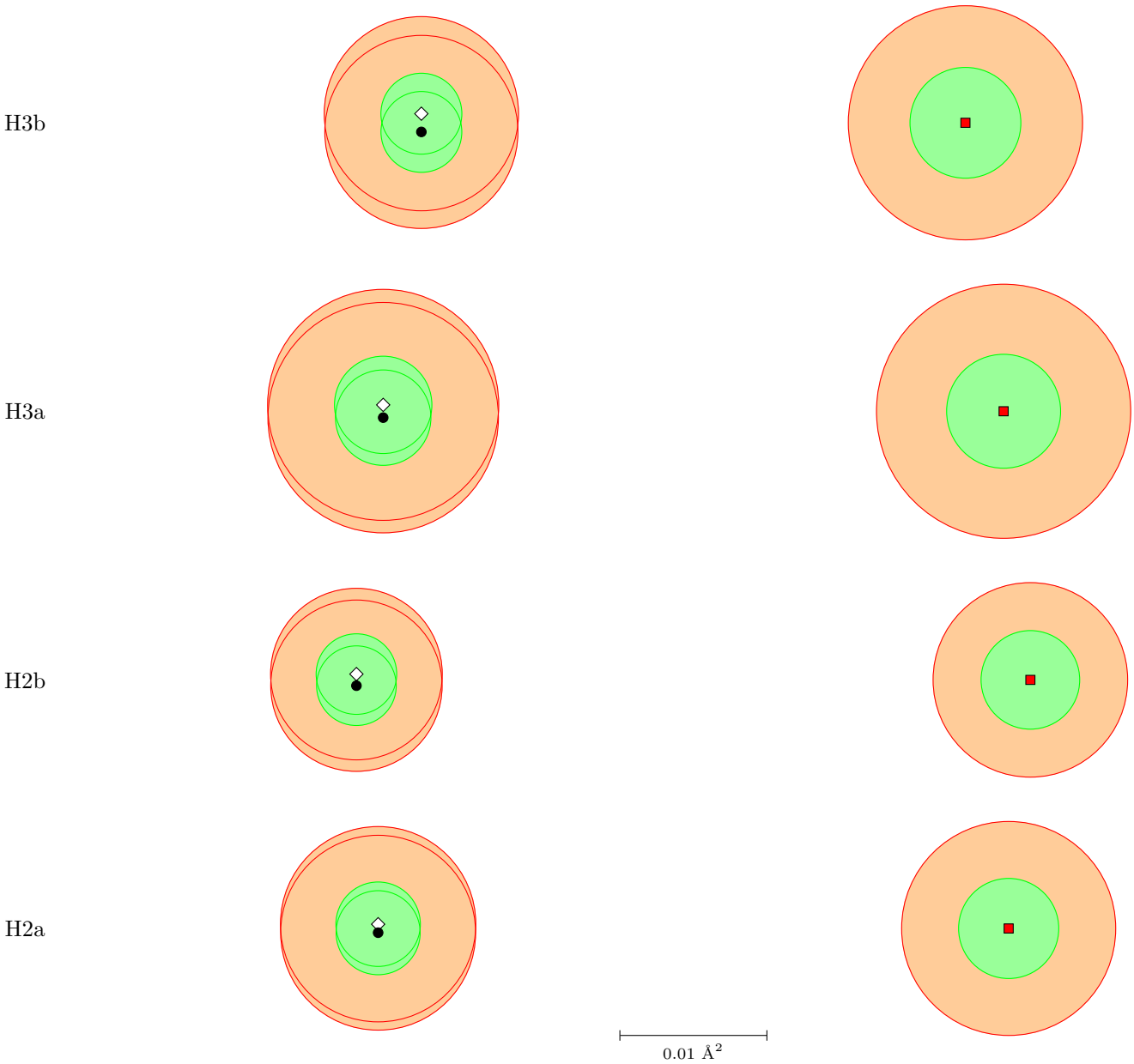

Figure S37: ADPs of the hydrogen atoms in $\mathbf{x}_{\mathrm{num}}$ (white ◇), $\mathbf{x}_{\mathrm{appr}}$ (black ●) and $\mathbf{x}_{\mathrm{spher}}$ (red ■), and their uncertainty balls. Green balls represent inner uncertainty balls and red balls represent outer uncertainty balls. (epoxide)

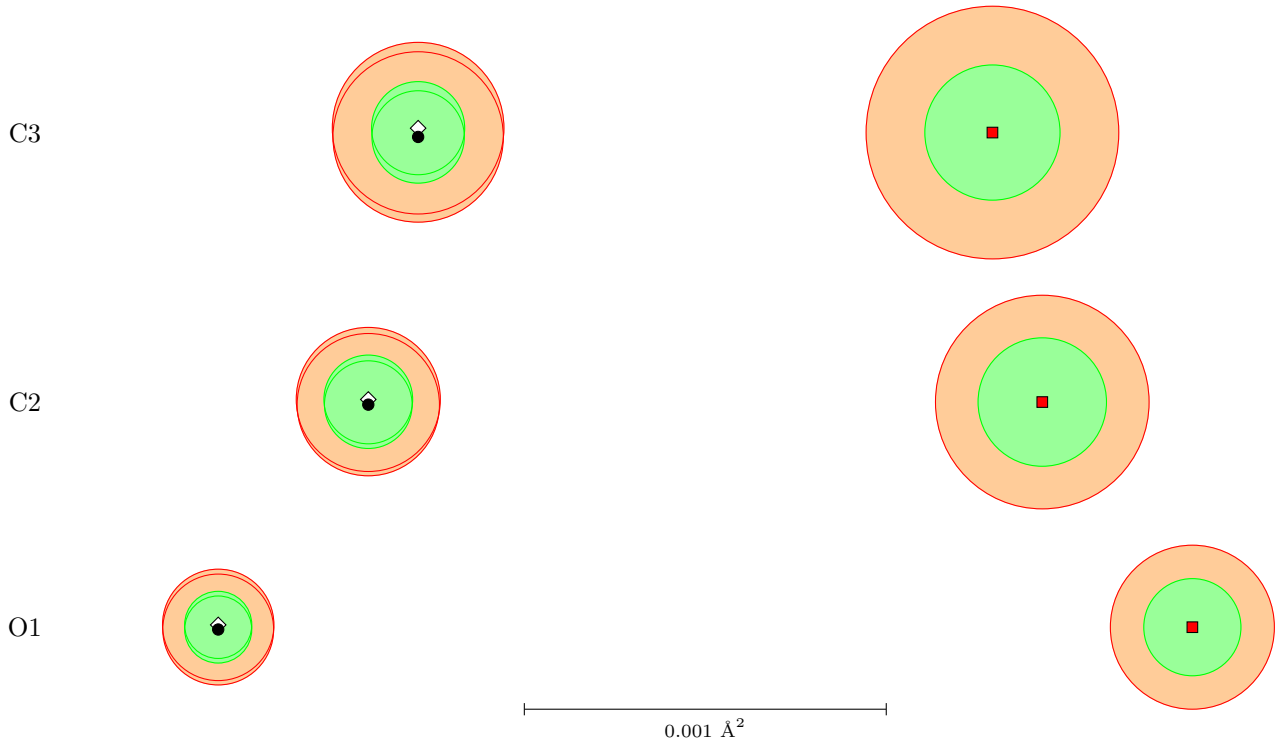

Figure S38: ADPs of the non-hydrogen atoms in $\mathbf{x}_{\text{num}}$ (white ◇), $\mathbf{x}_{\text{appr}}$ (black ●) and $\mathbf{x}_{\text{spher}}$ (red ■), and their uncertainty balls. Green balls represent inner uncertainty balls and red balls represent outer uncertainty balls. (epoxide)

	$\|A_{\text{num}} - A_{\text{spher}}\|$	$r(A_{\text{num}})$	$R(A_{\text{num}})$	$r(A_{\text{spher}})$	$R(A_{\text{spher}})$
A=O1	2.679e-03	9.246e-05	1.535e-04	1.338e-04	2.259e-04
A=C2	1.853e-03	1.222e-04	1.985e-04	1.769e-04	2.942e-04
A=H2a	4.276e-02	2.854e-03	6.604e-03	3.384e-03	7.235e-03
A=H2b	4.525e-02	2.723e-03	5.802e-03	3.333e-03	6.576e-03
A=C3	1.583e-03	1.282e-04	2.364e-04	1.862e-04	3.480e-04
A=H3a	4.159e-02	3.291e-03	7.811e-03	3.851e-03	8.591e-03
A=H3b	3.668e-02	2.736e-03	6.566e-03	3.746e-03	7.917e-03
	$\|A_{\text{num}} - A_{\text{appr}}\|$	$r(A_{\text{num}})$	$R(A_{\text{num}})$	$r(A_{\text{appr}})$	$R(A_{\text{appr}})$
A=O1	1.271e-05	9.246e-05	1.535e-04	9.236e-05	1.527e-04
A=C2	1.430e-05	1.222e-04	1.985e-04	1.207e-04	1.960e-04
A=H2a	5.745e-04	2.854e-03	6.604e-03	2.841e-03	6.589e-03
A=H2b	7.845e-04	2.723e-03	5.802e-03	2.692e-03	5.793e-03
A=C3	2.415e-05	1.282e-04	2.364e-04	1.272e-04	2.347e-04
A=H3a	8.633e-04	3.291e-03	7.811e-03	3.225e-03	7.790e-03
A=H3b	1.232e-03	2.736e-03	6.566e-03	2.733e-03	6.528e-03

Table S6: ADP difference (in Å^2) between atoms in $\mathbf{x}_{\text{num}}$, $\mathbf{x}_{\text{appr}}$, and $\mathbf{x}_{\text{spher}}$ and their comparison with uncertainty bounds. Red indicates a bound smaller than the difference, whilst green represents a bound larger than the difference (epoxide).

5.3 L-Alanine

	$\|A_{\text{num}} - A_{\text{spher}}\|$	$r(A_{\text{num}})$	$R(A_{\text{num}})$	$r(A_{\text{spher}})$	$R(A_{\text{spher}})$
A=N1	8.932e-04	2.510e-04	2.803e-04	4.813e-04	5.322e-04
A=H1a	1.076e-01	5.681e-03	7.998e-03	9.731e-03	1.310e-02
A=H1b	9.296e-02	5.480e-03	7.790e-03	8.991e-03	1.330e-02
A=H1c	7.742e-02	6.125e-03	6.901e-03	8.844e-03	1.754e-02
A=C1	2.624e-03	2.497e-04	2.920e-04	4.727e-04	5.498e-04
A=H1	9.049e-02	4.513e-03	6.608e-03	8.260e-03	1.059e-02
A=C2	2.788e-04	2.884e-04	3.335e-04	5.488e-04	6.320e-04
A=H2a	1.114e-01	5.375e-03	6.711e-03	9.842e-03	1.374e-02
A=H2b	1.281e-01	5.426e-03	7.179e-03	9.036e-03	1.253e-02
A=H2c	8.655e-02	5.073e-03	8.260e-03	8.993e-03	1.228e-02
A=C3	7.201e-04	2.465e-04	2.792e-04	4.656e-04	5.279e-04
A=O1	2.022e-03	2.022e-04	2.452e-04	3.811e-04	4.624e-04
A=O2	8.635e-04	2.043e-04	2.365e-04	3.863e-04	4.480e-04
	$\|A_{\text{num}} - A_{\text{appr}}\|$	$r(A_{\text{num}})$	$R(A_{\text{num}})$	$r(A_{\text{appr}})$	$R(A_{\text{appr}})$
A=N1	3.137e-05	2.510e-04	2.803e-04	2.499e-04	2.772e-04
A=H1a	3.723e-03	5.681e-03	7.998e-03	6.385e-03	8.082e-03
A=H1b	1.736e-03	5.480e-03	7.790e-03	6.129e-03	7.868e-03
A=H1c	4.864e-03	6.125e-03	6.901e-03	6.264e-03	8.056e-03
A=C1	7.121e-06	2.497e-04	2.920e-04	2.494e-04	2.930e-04
A=H1	2.242e-03	4.513e-03	6.608e-03	4.981e-03	6.509e-03
A=C2	1.933e-05	2.884e-04	3.335e-04	2.884e-04	3.308e-04
A=H2a	1.990e-03	5.375e-03	6.711e-03	5.785e-03	7.175e-03
A=H2b	2.074e-03	5.426e-03	7.179e-03	5.692e-03	7.394e-03
A=H2c	1.359e-03	5.073e-03	8.260e-03	5.429e-03	8.263e-03
A=C3	7.515e-06	2.465e-04	2.792e-04	2.470e-04	2.807e-04
A=O1	2.556e-05	2.022e-04	2.452e-04	2.036e-04	2.461e-04
A=O2	2.130e-05	2.043e-04	2.365e-04	2.055e-04	2.375e-04

Table S7: Positional difference (in Å) between atoms in $\mathbf{x}_{\text{num}}$, $\mathbf{x}_{\text{appr}}$, and $\mathbf{x}_{\text{spher}}$ and their comparison with uncertainty bounds. Red indicates a bound smaller than the difference, whilst green represents a bound larger than the difference (L-alanine).

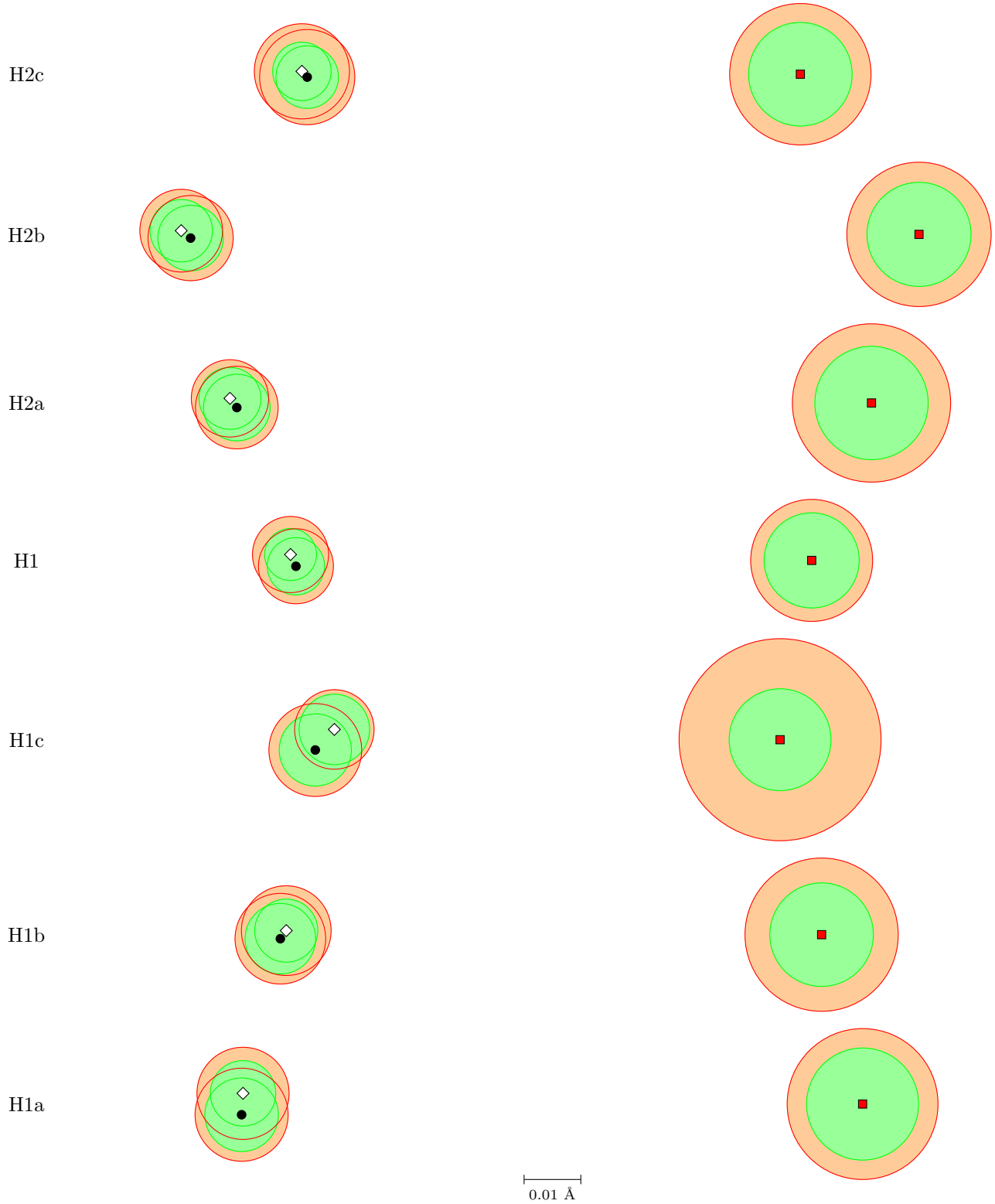

Figure S39: Positions of the hydrogen atoms in $\mathbf{x}_{\mathrm{num}}$ (white ◇), $\mathbf{x}_{\mathrm{appr}}$ (black ●) and $\mathbf{x}_{\mathrm{spher}}$ (red ■), and their uncertainty balls. Green balls represent inner uncertainty balls and red balls represent outer uncertainty balls. (L-alanine)

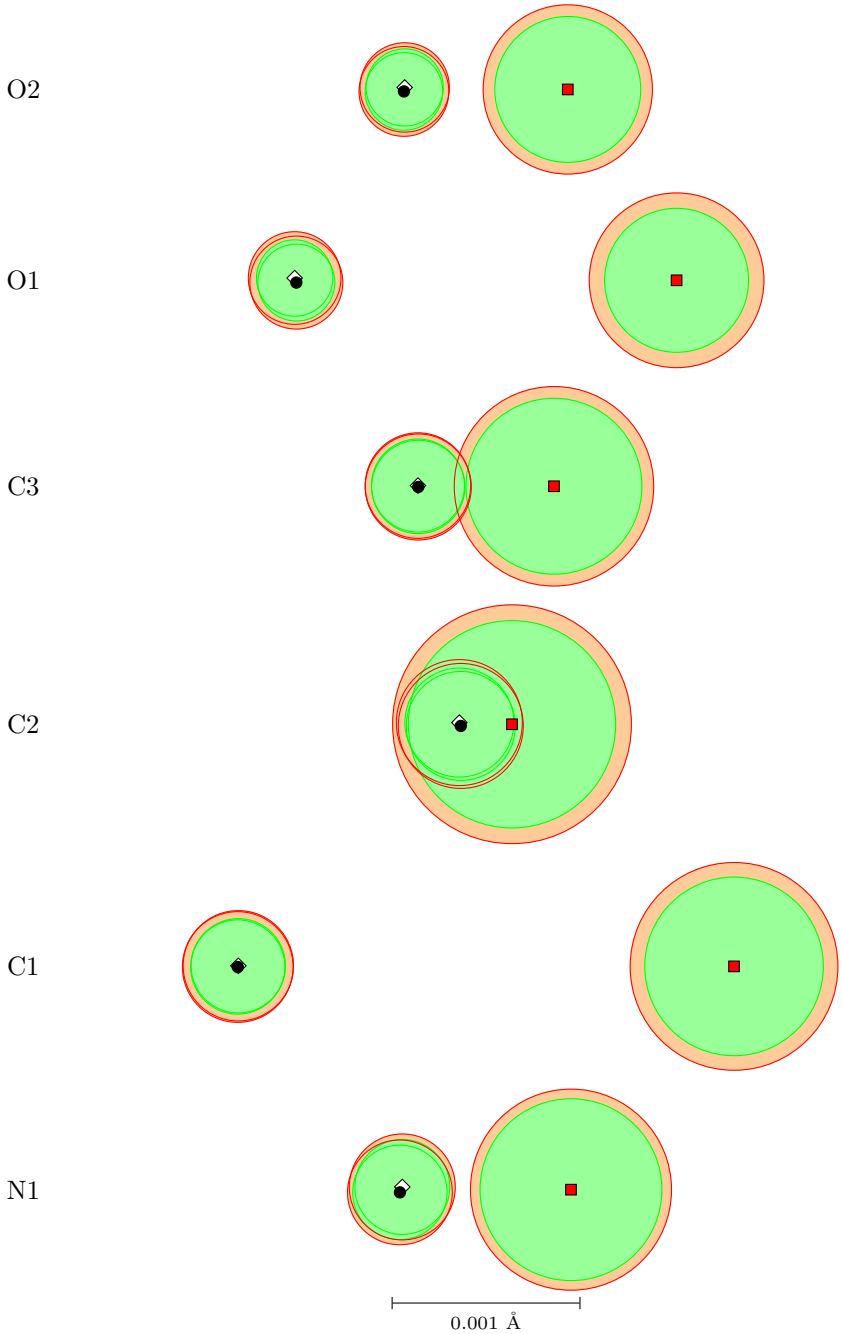

Figure S40: Positions of the non-hydrogen atoms in $\mathbf{x}_{\mathrm{num}}$ (white ◇), $\mathbf{x}_{\mathrm{appr}}$ (black ●) and $\mathbf{x}_{\mathrm{spher}}$ (red ■), and their uncertainty balls. Green balls represent inner uncertainty balls and red balls represent outer uncertainty balls. (L-alanine)

	$\|A_{\text{num}} - A_{\text{spher}}\|$	$r(A_{\text{num}})$	$R(A_{\text{num}})$	$r(A_{\text{spher}})$	$R(A_{\text{spher}})$
A=N1	6.211e-04	5.645e-05	9.182e-05	1.061e-04	1.702e-04
A=H1a	5.186e-02	2.876e-03	5.015e-03	4.265e-03	9.627e-03
A=H1b	2.991e-02	2.741e-03	4.949e-03	3.551e-03	8.364e-03
A=H1c	1.041e-01	2.765e-03	5.553e-03	3.631e-03	1.711e-02
A=C1	9.630e-04	6.001e-05	9.864e-05	1.139e-04	1.858e-04
A=H1	2.593e-02	2.216e-03	4.100e-03	3.224e-03	6.255e-03
A=C2	7.760e-04	6.677e-05	1.101e-04	1.265e-04	2.068e-04
A=H2a	2.999e-02	2.800e-03	5.158e-03	4.847e-03	9.370e-03
A=H2b	2.103e-02	2.766e-03	5.404e-03	4.173e-03	8.846e-03
A=H2c	3.582e-02	2.624e-03	5.858e-03	4.554e-03	8.060e-03
A=C3	1.002e-03	5.717e-05	9.384e-05	1.076e-04	1.770e-04
A=O1	9.886e-04	5.171e-05	8.777e-05	9.836e-05	1.653e-04
A=O2	7.778e-04	5.263e-05	8.164e-05	9.986e-05	1.533e-04
	$\|A_{\text{num}} - A_{\text{appr}}\|$	$r(A_{\text{num}})$	$R(A_{\text{num}})$	$r(A_{\text{appr}})$	$R(A_{\text{appr}})$
A=N1	1.197e-05	5.645e-05	9.182e-05	5.629e-05	8.993e-05
A=H1a	4.618e-04	2.876e-03	5.015e-03	2.833e-03	5.017e-03
A=H1b	3.718e-04	2.741e-03	4.949e-03	2.649e-03	4.917e-03
A=H1c	8.752e-04	2.765e-03	5.553e-03	2.701e-03	5.576e-03
A=C1	6.396e-06	6.001e-05	9.864e-05	5.981e-05	9.860e-05
A=H1	3.791e-04	2.216e-03	4.100e-03	2.219e-03	4.101e-03
A=C2	4.975e-06	6.677e-05	1.101e-04	6.665e-05	1.092e-04
A=H2a	1.276e-03	2.800e-03	5.158e-03	2.797e-03	5.173e-03
A=H2b	3.321e-04	2.766e-03	5.404e-03	2.728e-03	5.396e-03
A=H2c	1.033e-03	2.624e-03	5.858e-03	2.608e-03	5.892e-03
A=C3	6.221e-06	5.717e-05	9.384e-05	5.707e-05	9.384e-05
A=O1	5.503e-06	5.171e-05	8.777e-05	5.164e-05	8.777e-05
A=O2	4.666e-06	5.263e-05	8.164e-05	5.255e-05	8.167e-05

Table S8: ADP difference (in Å^2) between atoms in $\mathbf{x}_{\text{num}}$, $\mathbf{x}_{\text{appr}}$, and $\mathbf{x}_{\text{spher}}$ and their comparison with uncertainty bounds. Red indicates a bound smaller than the difference, whilst green represents a bound larger than the difference (L-alanine).

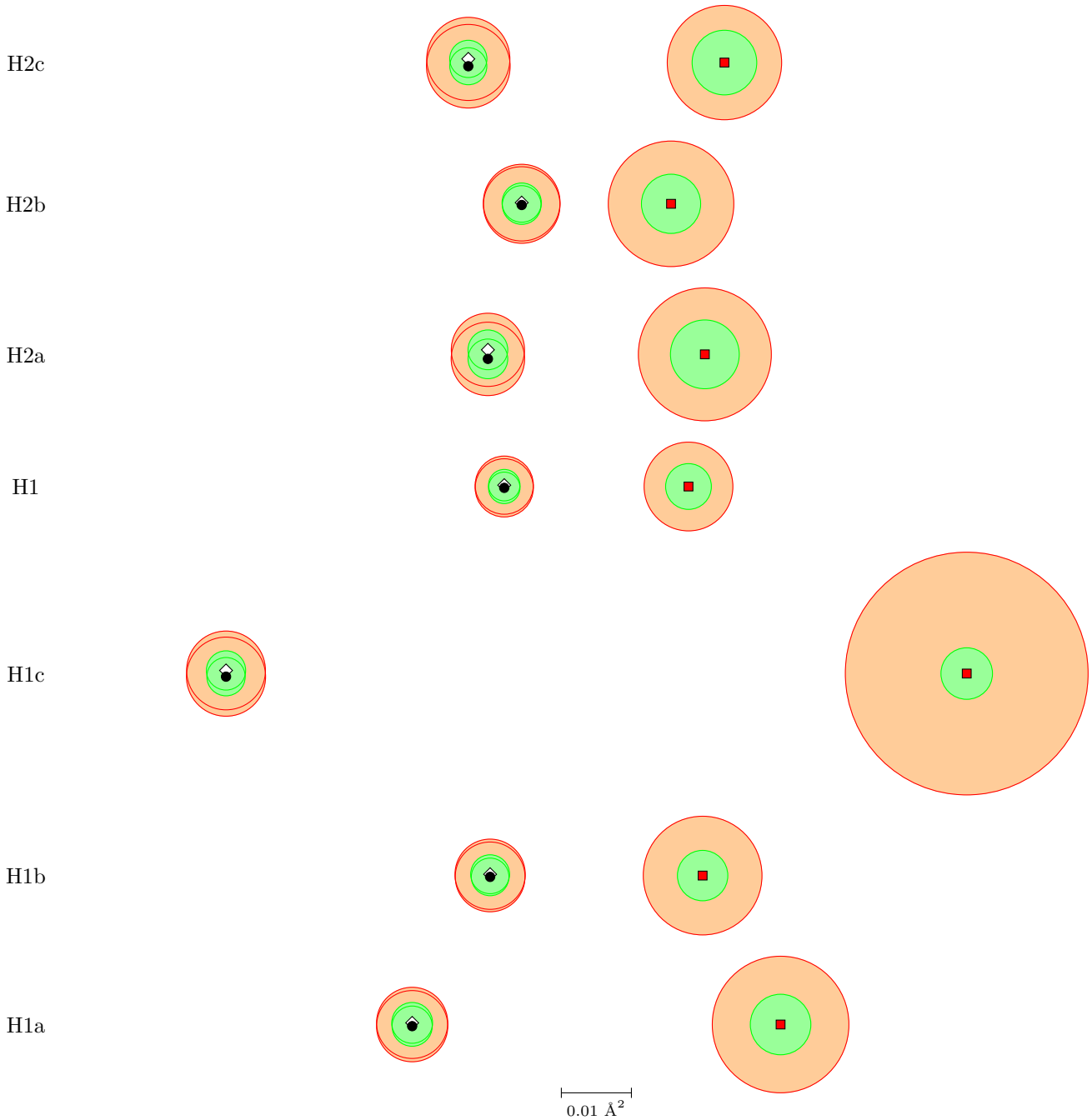

Figure S41: ADPs of the hydrogen atoms in $\mathbf{x}_{\mathrm{num}}$ (white ◇), $\mathbf{x}_{\mathrm{appr}}$ (black ●) and $\mathbf{x}_{\mathrm{spher}}$ (red ■), and their uncertainty balls. Green balls represent inner uncertainty balls and red balls represent outer uncertainty balls. (L-alanine)

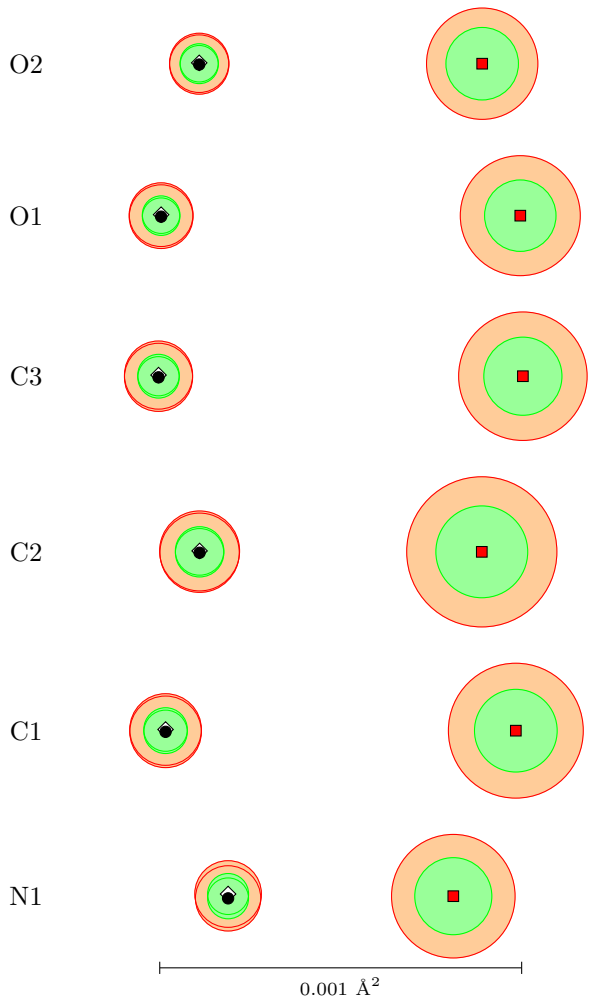

Figure S42: ADPs of the non-hydrogen atoms in $\mathbf{x}_{\mathrm{num}}$ (white ◇), $\mathbf{x}_{\mathrm{appr}}$ (black ●) and $\mathbf{x}_{\mathrm{spher}}$ (red ■), and their uncertainty balls. Green balls represent inner uncertainty balls and red balls represent outer uncertainty balls. (L-alanine)

6 Conclusion & Outlook

6.1 Neutron data

Here we present additional comparison with neutron data in Figures S43 to S46. Recall that the purple dot now represents the atom in the neutron model.

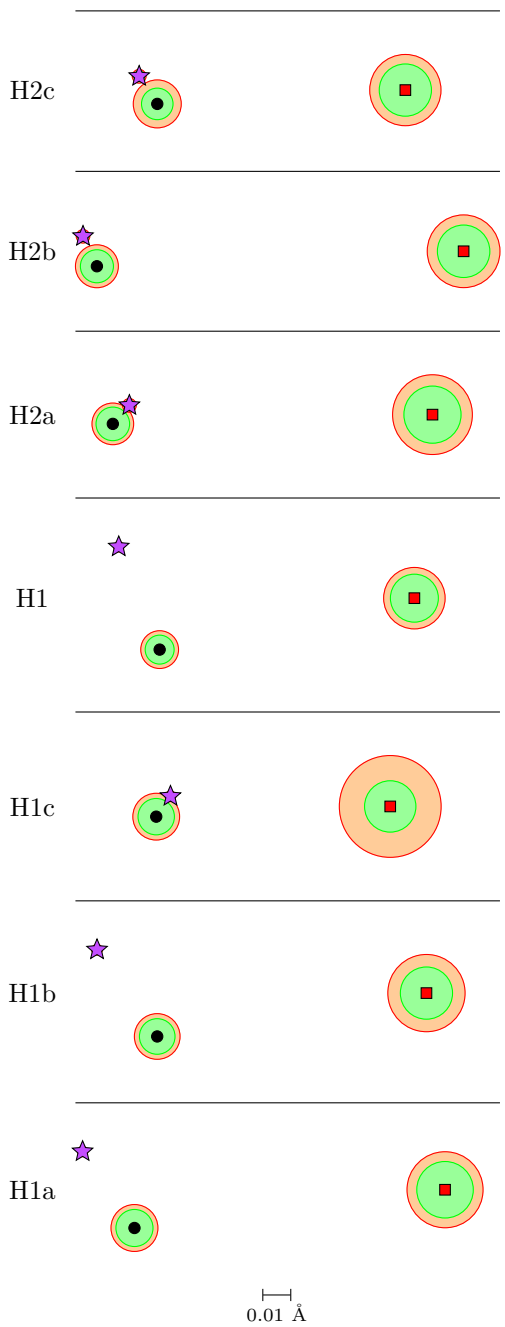

Figure S43: Positions of the hydrogen atoms in $\mathbf{x}_{\text{neutron}}$ (purple ★), $\mathbf{x}_{\text{appr}}$ (black ●) and $\mathbf{x}_{\text{spher}}$ (red ■), and their uncertainty balls. Green balls represent inner uncertainty balls and red balls represent outer uncertainty balls. (L-alanine)

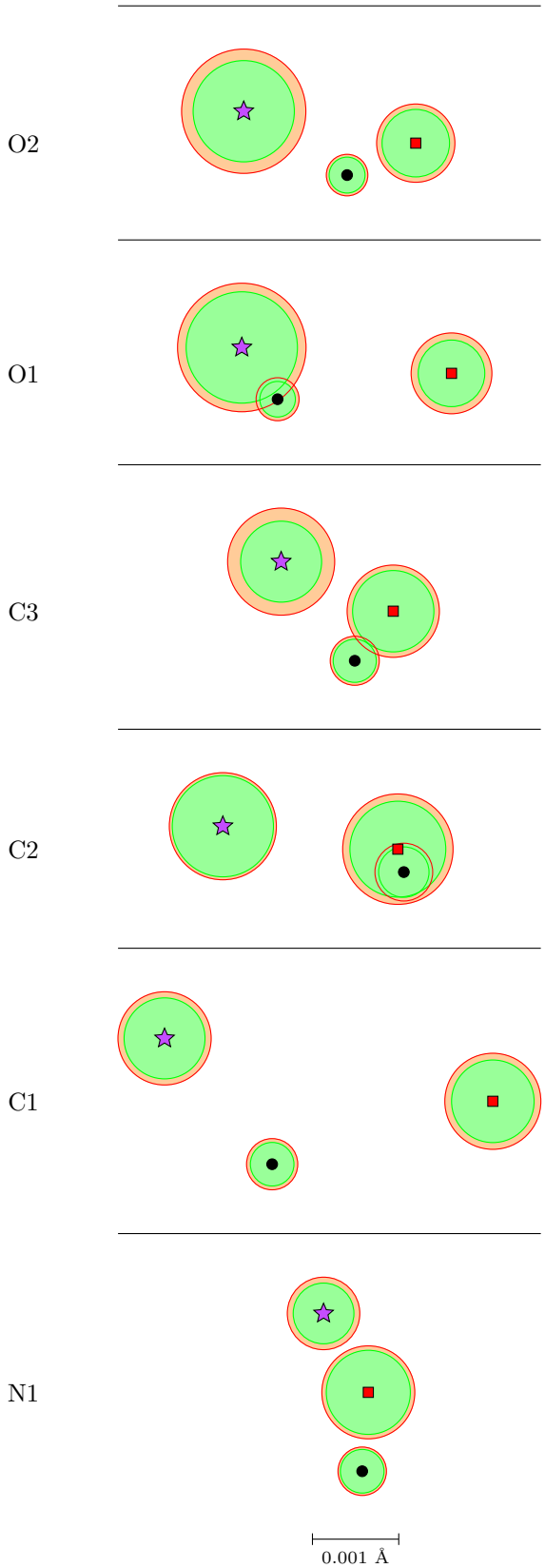

Figure S44: Positions of the non-hydrogen atoms in $\mathbf{x}_{\text{neutron}}$ (purple ★), $\mathbf{x}_{\text{appr}}$ (black ●) and $\mathbf{x}_{\text{spher}}$ (red ■), and their uncertainty balls. Green balls represent inner uncertainty balls and red balls represent outer uncertainty balls. (L-alanine)

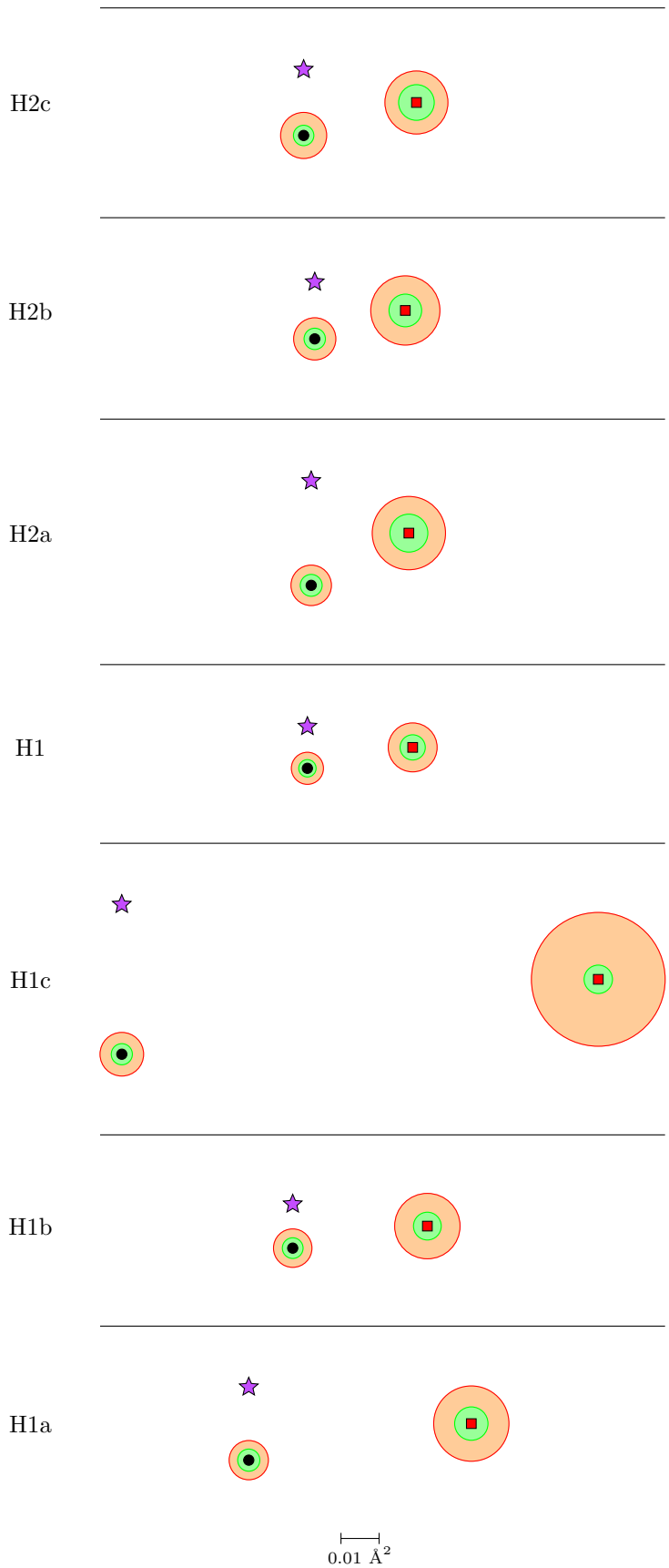

Figure S45: ADPs of the hydrogen atoms in $\mathbf{x}_{\text{neutron}}$ (purple ★), $\mathbf{x}_{\text{appr}}$ (black ●) and $\mathbf{x}_{\text{spher}}$ (red ■), and their uncertainty balls. Green balls represent inner uncertainty balls and red balls represent outer uncertainty balls. (L-alanine)

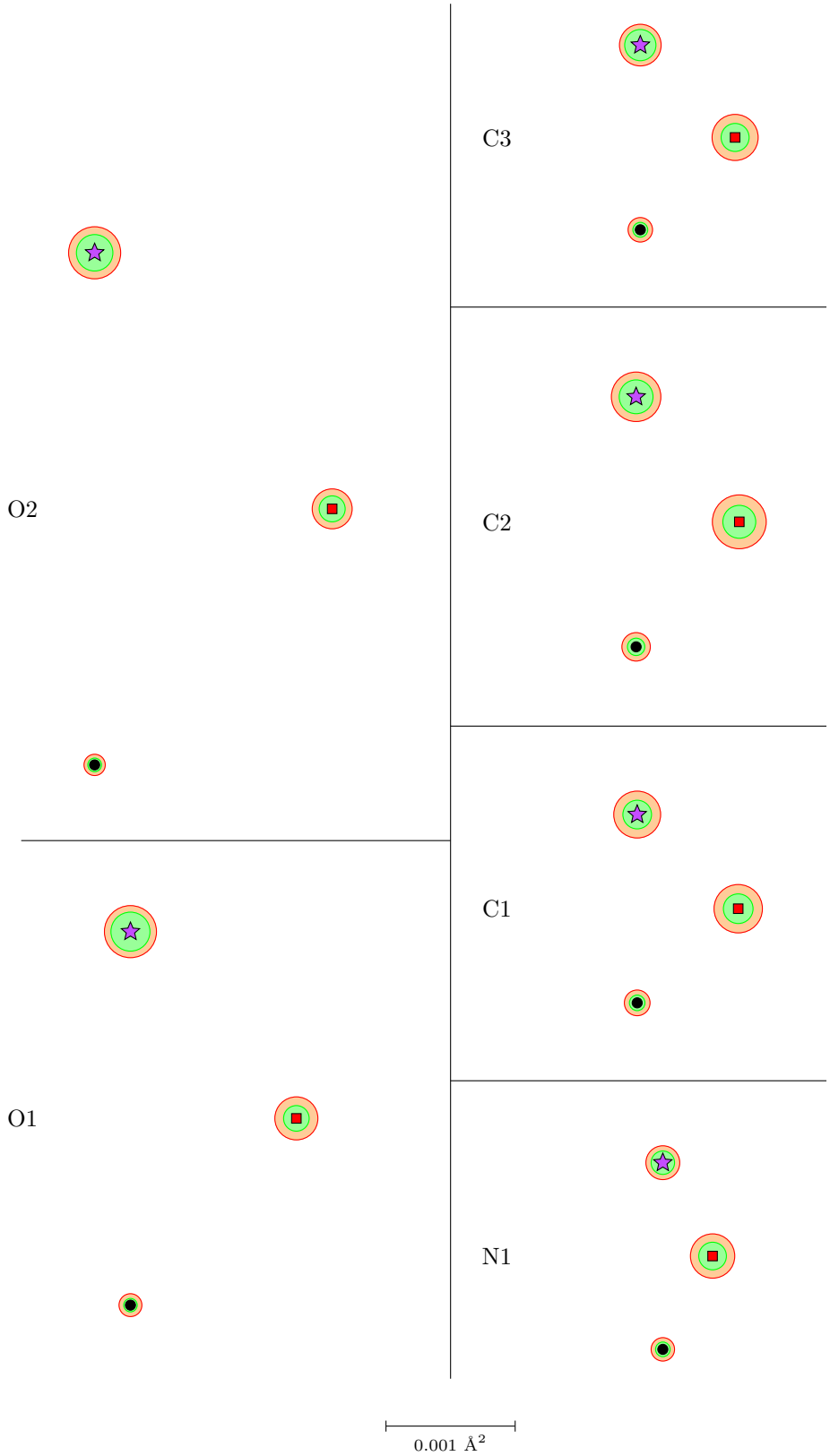

Figure S46: ADPs of the non-hydrogen atoms in $\mathbf{x}_{\text{neutron}}$ (purple ★), $\mathbf{x}_{\text{appr}}$ (black ●) and $\mathbf{x}_{\text{spher}}$ (red ■), and their uncertainty balls. Green balls represent inner uncertainty balls and red balls represent outer uncertainty balls. (L-alanine)

B Uncertainty balls

B.1 The matrix J for ammonia

The matrix 'J' for ammonia, which expands the model vector $\mathbf{x}$ to the full vector $\mathbf{y}$ of all crystallographic parameters, is presented in Equation (S1).

$$J = \begin{bmatrix} J_0 & 0_{3,9} \\ 0_{9,9} & \mathrm{Id}_9 \end{bmatrix} \tag{S1}$$

with $0_{p,q}$ the $p \times q$ matrix with all entries equal to 0, Id_p the identity matrix of size p and

$$J_0 = \begin{bmatrix} 1 & 1 & 1 & 0 & 0 & 0 & 0 & 0 & 0 \\ 0 & 0 & 0 & 1 & 1 & 1 & 0 & 0 & 0 \\ 0 & 0 & 0 & 0 & 0 & 0 & 1 & 1 & 1 \end{bmatrix}.$$